Fig. 4

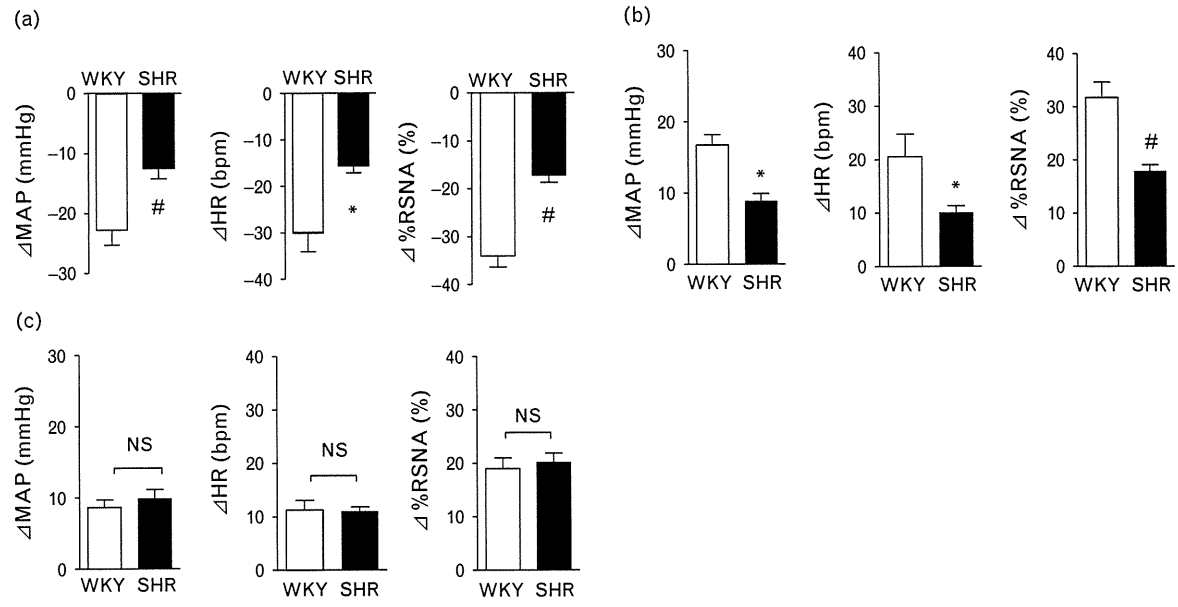

Comparison of responses of mean arterial pressure (MAP), heart rate (HR), and renal sympathetic nerve activity (RSNA) (%baseline) in 12-week-old Wistar–Kyoto (WKY) and spontaneously hypertensive rats to (a) unilateral injection of neuregulin-1β (2.5 pmol); (b) bilateral injection of AG825 (1.0 pmol); and (c) injection of AG1478 (1.0 pmol) into the rostral ventrolateral medulla. Values are expressed as mean ± SEM. $^{*}P < 0.05$; $^{\#}P < 0.01$ (vs. WKY rats, $n = 5$ per injection).

receptor antagonist as well as the ErbB4 receptor antagonist into the RVLM increased arterial pressure, HR, and RSNA. These data suggest that NRG-1/ErbB signaling in the RVLM is involved in regulating resting blood pressure. The depressor response to NRG-1 was nearly completely blocked when both ErbB2 and ErbB4 receptor blockers were administered. We cannot exclude the possibility that the ErbB3 receptors might also be involved in the depressor response to NRG-1 because NRG-1 stimulation could induce ErbB2/ErbB3 heterodimer or ErbB3 homodimer formation. We did not examine the effect of ErbB3 inhibition because the ErbB3 receptor antagonist is commercially not available. However, the role of the ErbB3 receptor in the NRG-1-induced hypotensive response in the RVLM is probably not that strong based on the results obtained using ErbB2 and ErbB4 receptor antagonists. It has been reported that only NRG-1, ErbB2, and ErbB4 are present in synapse-rich regions [32]. It should be noted that it has also been reported that peripheral NRG-1 affects cardiomyocytes, leading to negative inotropic effects [19]. Our findings are evoked by the agents of their central effects because the amount of the agents used in the present study is very small and directly administered into the RVLM. In fact, we did not find blood pressure and HR changes when the same amount of agents was administered systemically in Wistar rats.

It is possible that synaptic function alteration in the RVLM might be involved in the NRG-1-induced hypotensive response. The depressor response to NRG-1 injection into the RVLM was attenuated by the blockade of the GABA-A receptors. This supports the hypothesis that NRG-1 in the RVLM increases GABA, the major inhibitory neurotransmitter, and releases and/or augments GABA-A receptor activity. The pressor response to L-glutamate, the major excitatory neurotransmitter, was also attenuated prior to the injection of NRG-1 into the RVLM. This suggests that *N*-methyl-D-aspartic acid (NMDA) and/or non-NMDA response to L-glutamate is attenuated by NRG-1 stimulation. Because the major neurotransmitters involved in regulating the activity of RVLM neurons include glutamate and GABA [18], alteration of synaptic transmission induced by L-glutamate and GABA is important for regulating SNA [17]. NRG-1 and ErbB receptors are extensively distributed in the brain, including the medulla, and they exist in neurons, glia, and oligodendrocytes [3]. Also, it has been reported that glutamate and GABA receptors colocalizes with ErbB receptors in postsynaptic lesions [6–9]. Several studies have shown that the NRG-1/ErbB pathway is involved in the regulation of postsynaptic glutamate receptor function and presynaptic release of GABA, although these functions have not been determined for the RVLM [11,12,33,34]. For example, NRG-1 significantly enhances the depolarization-induced release of GABA in hippocampal neurons [11] and inhibits NMDA receptor currents in prefrontal cortex neurons [12,33,34]. Determining whether the actions are presynaptic vs. postsynaptic is difficult. We did not address

Fig. 5

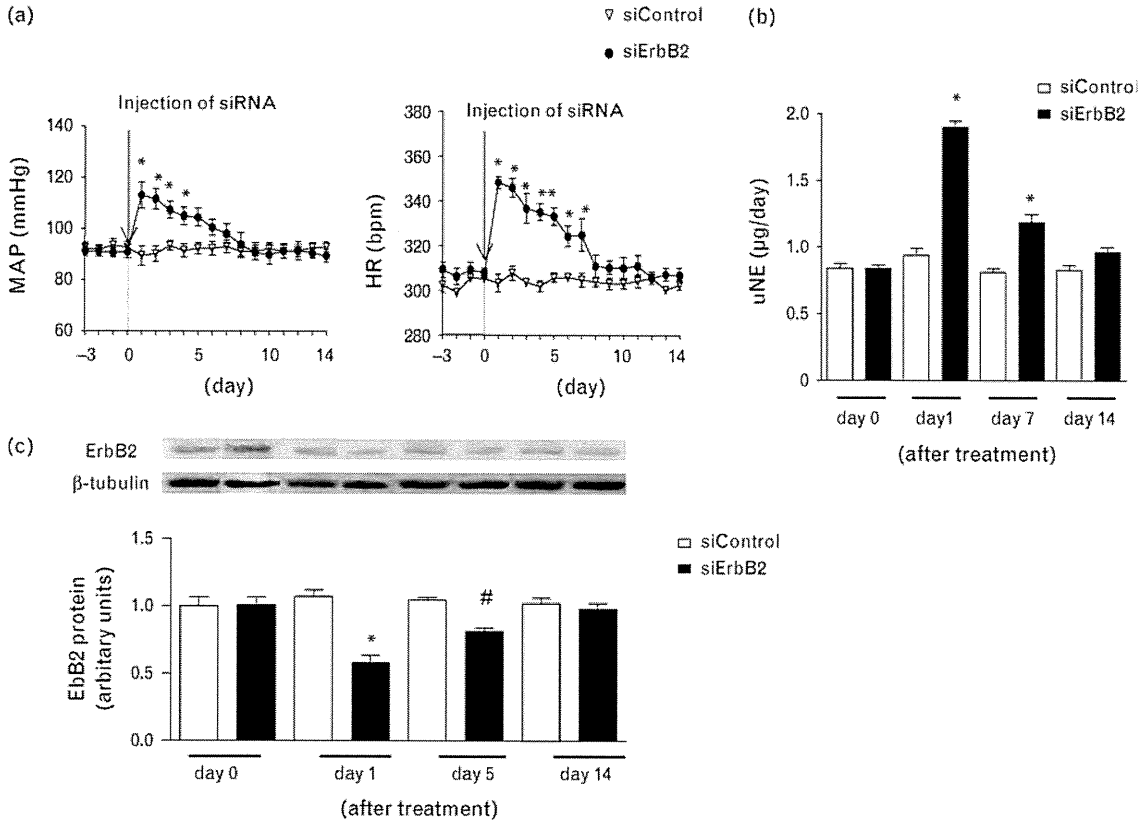

Effect of chronic ErbB2 receptor inhibition in the rostral ventrolateral medulla (RVLM) of Wistar–Kyoto rats on mean arterial pressure (MAP), heart rate (HR), and sympathetic nerve activity. (a) Effect of local administration of ErbB2 small-interference RNA (siRNA) (siErbB2) and control siRNA (siControl) into the RVLM on MAP and HR. $^{*}P < 0.05$ (vs. day-matched siControl treatment groups, $n = 5$ for each). (b) Group data for urinary norepinephrine excretion (uNE) at day 0 (before treatment), 1, 7, and 14 after starting the treatment (μg/day). $^{*}P < 0.01$ vs. siControl day 0 ($n = 5$ for each). (c) Western blot of ErbB2 in the RVLM in the siErbB2 treatment and siControl treatment groups. Western blot was performed at day 0 (before treatment), 1, 5, and 14 after starting the treatment. The densitometric average was normalized to the values obtained from the analysis of β-tubulin as internal control. $^{*}P < 0.01$; $^{\#}P < 0.05$ (vs. day0, $n = 5$ for each). Expressions are shown relative to that on day 0, which was assigned a value of 1. Values are expressed as mean ± SEM.

which cells were responsible for our observations. Further studies are necessary to clarify the precise mechanisms involved.

In addition to the blood pressure-lowering effect of the NRG-1/ErbB signaling in the RVLM through sympathoinhibition, we found that this signaling in the RVLM is impaired in SHRs compared with that in WKY rats. Particularly, reduced ErbB2 receptor expression levels in the RVLM of SHRs occurred during the prehypertensive age and persisted through the established hypertensive age of SHRs. Although NRG-1 and ErbB receptors are expressed in the brain, we did not observe reduced ErbB2 expression levels in other areas of the brain in SHRs (cerebral cortex and hypothalamus). Importantly, the depressor response to NRG-1 and the pressor response to the ErbB2 antagonist were attenuated in SHRs compared with responses in WKY rats. However, the pressor response to ErbB4 inhibitor did not differ between SHRs and WKY rats. Thus, we suggest that the reduction of ErbB2 receptors in the RVLM might contribute to the hypertensive state of SHRs.

On the basis of these findings, we further investigated whether a reduction in ErbB2 expression in the RVLM contributes to increased blood pressure in the conscious state. We inhibited ErbB2 expression in the RVLM of WKY rats using siRNAs. In this experiment, we used the AteloGene kit to deliver siErbB2 into the RVLM. AteloGene is a commercial kit used to locally administer siRNA into tissues *in vivo*. It has no toxicity and forms a gel in the body [35]. Thus, siRNA is maintained at the administration site [35]. Our findings indicate that reducing ErbB2 receptor expression levels in the RVLM increases blood pressure and HR and is associated with sympathoexcitation. These findings also suggest a dysfunction in NRG-1/ErbB signaling; reduction in ErbB2 levels in the RVLM might contribute to the neural mechanisms of hypertension in SHRs.

In conclusion, our findings indicate that the NRG-1/ErbB signaling in the RVLM exerts antihypertensive effects by reducing SNA in normotensive rats. Furthermore, impairment of NRG-1/ErbB signaling in the RVLM due to reduced levels of endogenous ErbB2 is a possible neural mechanism of hypertension in SHRs.

Acknowledgements

This study was supported by Grants-in-Aid for Scientific Research from the Japan Society for the Promotion of Science and a Grant from the Mitsubishi Pharma Research Foundation.

Conflicts of interest

There are no conflicts of interest.

References

1 Lemmens K, Doggen K, De Keulenaer GW. Role of neuregulin-1/ErbB signaling in cardiovascular physiology and disease: implications for therapy of heart failure. *Circulation* 2007; **116**:954–960.
2 Melenhorst WB, Mulder GM, Xi Q, Hoenderop JG, Kimura K, Eguchi S, van Goor H. Epidermal growth factor receptor signaling in the kidney: key roles in physiology and disease. *Hypertension* 2008; **52**:987–993.
3 Mei L, Xiong WC. Neuregulin 1 in neural development, synaptic plasticity and schizophrenia. *Nat Rev Neurosci* 2008; **9**:437–452.
4 Falls DL. Neuregulins: functions, forms, and signaling strategies. *Exp Cell Res* 2003; **284**:14–30.
5 Rio C, Rieff HI, Qi P, Khurana TS, Corfas G. Neuregulin and erbB receptors play a critical role in neuronal migration. *Neuron* 1997; **19**:39–50.
6 Gerecke KM, Wyss JM, Karavanova I, Buonanno A, Carroll SL. ErbB transmembrane tyrosine kinase receptors are differentially expressed throughout the adult rat central nervous system. *J Comp Neurol* 2001; **433**:86–100.
7 Thompson M, Lauderdale S, Webster MJ, Chong VZ, McClintock B, Saunders R, Weickert CS. Widespread expression of ErbB2, ErbB3 and ErbB4 in nonhuman primate brain. *Brain Res* 2007; **1139**:95–109.
8 Fox IJ, Kornblum HI. Developmental profile of ErbB receptors in murine central nervous system: implications for functional interactions. *J Neurosci Res* 2005; **79**:584–597.
9 Abe Y, Namba H, Zheng Y, Nawa H. In situ hybridization reveals developmental regulation of ErbB1-4 mRNA expression in mouse midbrain: implication of ErbB receptors for dopaminergic neurons. *Neuroscience* 2009; **161**:95–110.
10 Brinkmann BG, Agarwal A, Sereda MW, Garratt AN, Muller T, Wende H, *et al.* Neuregulin-1/ErbB signaling serves distinct functions in myelination of the peripheral and central nervous system. *Neuron* 2008; **59**:581–595.
11 Woo RS, Li XM, Tao Y, Carpenter-Hyland E, Huang YZ, Weber J, *et al.* Neuregulin-1 enhances depolarization-induced GABA release. *Neuron* 2007; **54**:599–610.
12 Li B, Woo RS, Mei L, Malinow R. The neuregulin-1 receptor erbB4 controls glutamatergic synapse maturation and plasticity. *Neuron* 2007; **54**:583–597.
13 Schmid RS, McGrath B, Berechid BE, Boyles B, Marchionni M, Sestan N, Anton ES. Neuregulin 1-erbB2 signaling is required for the establishment of radial glia and their transformation into astrocytes in cerebral cortex. *Proc Natl Acad Sci U S A* 2003; **100**:4251–4256.
14 Campos RR, Bergamaschi CT. Neurotransmission alterations in central cardiovascular control in experimental hypertension. *Curr Hypertens Rev* 2006; **2**:193–198.
15 Guyenet PG. The sympathetic control of blood pressure. *Nat Rev Neurosci* 2006; **7**:335–346.
16 Hirooka Y, Sagara Y, Kishi T, Sunagawa K. Oxidative stress and central cardiovascular regulation. *Circ J* 2010; **74**:827–835.
17 Sved AF, Ito S, Sved JC. Brainstem mechanisms of hypertension: role of the rostral ventrolateral medulla. *Curr Hypertens Rep* 2003; **5**:262–268.
18 Schreihofer AM, Guyenet PG. The baroreflex and beyond: control of sympathetic vasomotor tone by GABAergic neurons in the ventrolateral medulla. *Clin Exp Pharmacol Physiol* 2002; **29**:514–521.
19 Lemmens K, Fransen P, Sys SU, Brutsaert DL, De Keulenaer GW. Neuregulin-1 induces a negative inotropic effect in cardiac muscle: role of nitric oxide synthase. *Circulation* 2004; **109**:324–326.
20 Zhu WZ, Xie Y, Moyes KW, Gold JD, Askari B, Laflamme MA. Neuregulin/ErbB signaling regulates cardiac subtype specification in differentiating human embryonic stem cells. *Circ Res* 2010; **107**:776–786.
21 Tsai CM, Levitzki A, Wu LH, Chang KT, Cheng CC, Gazit A, Perng RP. Enhancement of chemosensitivity by tyrphostin AG825 in high-p185(neu) expressing nonsmall cell lung cancer cells. *Cancer Res* 1996; **56**:1068–1074.
22 Osherov N, Gazit A, Gilon C, Levitzki A. Selective inhibition of the epidermal growth factor and HER2/neu receptors by tyrphostins. *J Biol Chem* 1993; **268**:11134–11142.
23 Ishii Y, Fujimoto S, Fukuda T. Gefitinib prevents bleomycin-induced lung fibrosis in mice. *Am J Respir Crit Care Med* 2006; **174**:550–556.
24 Gajendran N, Kapfhammer JP, Lain E, Canepari M, Vogt K, Wisden W, Brenner HR. Neuregulin signaling is dispensable for NMDA- and GABA(A)-receptor expression in the cerebellum in vivo. *J Neurosci* 2009; **29**:2404–2413.
25 Choi BH, Choi JS, Rhie DJ, Yoon SH, Min DS, Jo YH, *et al.* Direct inhibition of the cloned Kv1.5 channel by AG-1478, a tyrosine kinase inhibitor. *Am J Physiol Cell Physiol* 2002; **282**:C1461–C1468.
26 Kishi T, Hirooka Y, Sakai K, Shigematsu H, Shimokawa H, Takeshita A. Overexpression of eNOS in the RVLM causes hypotension and bradycardia via GABA release. *Hypertension* 2001; **38**:896–901.
27 Hirooka Y, Polson JW, Dampney RA. Pressor and sympathoexcitatory effects of nitric oxide in the rostral ventrolateral medulla. *J Hypertens* 1996; **14**:1317–1324.
28 Horiuchi J, Dampney RA. Evidence for tonic disinhibition of RVLM sympathoexcitatory neurons from the caudal pressor area. *Auton Neurosci* 2002; **99**:102–110.
29 Kishi T, Hirooka Y, Kimura Y, Ito K, Shimokawa H, Takeshita A. Increased reactive oxygen species in rostral ventrolateral medulla contribute to neural mechanisms of hypertension in stroke-prone spontaneously hypertensive rats. *Circulation* 2004; **109**:2357–2362.
30 Grazette LP, Boecker W, Matsui T, Semigran M, Force TL, Hajjar RJ, Rosenzweig A. Inhibition of ErbB2 causes mitochondrial dysfunction in cardiomyocytes: implications for herceptin-induced cardiomyopathy. *J Am Coll Cardiol* 2004; **44**:2231–2238.
31 Sakai K, Hirooka Y, Matsuo I, Eshima K, Shigematsu H, Shimokawa H, Takeshita A. Overexpression of eNOS in NTS causes hypotension and bradycardia in vivo. *Hypertension* 2000; **36**:1023–1028.
32 Chaudhury AR, Gerecke KM, Wyss JM, Morgan DG, Gordon MN, Carroll SL. Neuregulin-1 and erbB4 immunoreactivity is associated with neuritic plaques in Alzheimer disease brain and in a transgenic model of Alzheimer disease. *J Neuropathol Exp Neurol* 2003; **62**:42–54.
33 Gu Z, Jiang Q, Fu AK, Ip NY, Yan Z. Regulation of NMDA receptors by neuregulin signaling in prefrontal cortex. *J Neurosci* 2005; **25**:4974–4984.
34 Fischbach GD. NRG1 and synaptic function in the CNS. *Neuron* 2007; **54**:495–497.
35 Minakuchi Y, Takeshita F, Kosaka N, Sasaki H, Yamamoto Y, Kouno M, *et al.* Atelocollagen-mediated synthetic small interfering RNA delivery for effective gene silencing in vitro and in vivo. *Nucleic Acids Res* 2004; **32**:e109.

Clinical and Experimental Hypertension, 33(4):240–245, (2011)

ISSN 1064-1963 print/1525-6006 online
DOI: 10.3109/10641963.2011.583969

informa
healthcare

Calorie Restriction inhibits Sympathetic Nerve Activity via Anti-Oxidant Effect in the Rostral Ventrolateral Medulla of Obesity-Induced Hypertensive Rats

Takuya Kishi, Yoshitaka Hirooka, Kiyohiro Ogawa, Satomi Konno, Kenji Sunagawa

Department of Advanced Therapeutics for Cardiovascular Diseases, Department of Cardiovascular Medicine, Kyushu University Graduate School of Medical Sciences, Fukuoka, Japan

Abstract

In the patients and animals with metabolic syndrome (MetS), sympathetic nerve activity (SNA) is increased. We have demonstrated that oxidative stress in the rostral ventrolateral medulla (RVLM), a vasomotor center in the brainstem, increases SNA. The aim of the present study was to determine whether calorie restriction inhibits SNA via anti-oxidant effect in the RVLM of obesity-induced obesity rats. Male Sprague-Dawley rats were fed on a high-fat diet and segregated into obesity-prone (OP) showing a MetS profile and obesity-resistant (OR) after 13 weeks. Obesity-prone was divided into OP treated with calorie restriction (CR-OP) for 8 weeks and control (CTR-OP). Systolic blood pressure (SBP), heart rate (HR), SNA, and thiobarbituric acid-reactive substances (TBARS) levels as a marker of oxidative stress in the RVLM were significantly higher and the depressor effects due to the microinjection of tempol, a superoxide dismutase mimetic into the RVLM, were significantly greater in OP than in OR. Body weight was significantly lower in CR-OP than in CTR-OP. SBP, HR, SNA, TBARS, and the depressor effects due to the microinjection of tempol into the RVLM were significantly lower in CR-OP than in CTR-OP. These results suggest that calorie restriction inhibits SNA via anti-oxidant effect in the RVLM of obesity-induced obesity rats.

keywords: calorie restriction, metabolic syndrome, sympathetic nerve activity, oxidative stress, brain

INTRODUCTION

Metabolic syndrome (MetS), a complex of highly debilitating disorders that consist of hypertension, diabetes mellitus, and dyslipidemia, is associated with the development of visceral obesity (1). Previous study indicated that sympathetic activation may be involved in obesity-induced hypertension (2). In obesity-induced hypertension, increased oxidative stress in the hypothalamus may contribute to the progression of hypertension through central sympatho-excitation (3). Several studies have also suggested that oxidative stress may be the unifying mechanisms underlying the development of hypertension in obesity (4–6). In preclinical testing, one non-pharmacologic approach that was shown to be beneficial in a variety of cardiovascular diseases is long-term calorie restriction (CR) (7–9). Although long-term CR has been shown to prevent increases in blood pressure (BP) in nonobese hypertensive rats, little is known about the mechanisms responsible for these observations.

Rostral ventrolateral medulla (RVLM) in the brainstem is the vasomotor center that determines basal sympathetic nerve activity (SNA), and the functional integrity of the RVLM is essential for the maintenance of basal vasomotor tone (10, 11). We have demonstrated that oxidative stress in the RVLM produced by angiotensin II type 1 receptor (AT_1R) increases the SNA (12, 13), and that nitric oxide (NO) in the RVLM decreases the SNA (14–17). Our other reports have suggested that the imbalance between oxidative stress and NO in the brain cause cardiovascular diseases (18–22). Previous reports have suggested that oxidative stress in the hypothalamus cause sympatho-excitation in the obesity-induced hypertensive rats (3), and that neurons in the RVLM contribute to elevated sympathetic outflow in a rodent model of diet-induced obesity (23). However, it has not been determined whether the calorie restriction decreases SNA via anti-oxidant in the RVLM of obesity-induced hypertensive rats.

Address correspondence to Takuya Kishi, MD, PhD, FAHA, Department of Advanced Therapeutics for Cardiovascular Diseases, Department of Cardiovascular Medicine, Kyushu University Graduate School of Medical Sciences, 3-1-1 Maidashi, Higashi-ku, Fukuoka 812-8582, Japan. E-mail: tkishi@cardiol.med.kyushu-u.ac.jp

Received 31 August 2010; revised 9 November 2010; accepted 12 November 2010.

Therefore, the aim of the present study was to investigate the effect of calorie restriction on the SNA and oxidative stress in the RVLM of obesity-induced hypertensive rats. To determine this aim, we measured BP, heart rate (HR), urine norepinephrine excretion as a parameter of SNA, and oxidative stress in the RVLM. Furthermore, to inhibit the oxidative stress in the RVLM locally, we microinjected tempol, a superoxide dismutase (SOD) mimetic, into the RVLM. Previously, we performed the same experiments in the hypertensive model rats, in which the microinjection of tempol into the RVLM caused depressor and bradycardia (12). In that experiment, we also performed the overexpression of Mn-SOD into the bilateral RVLM of hypertensive rats, and inhibited the oxidative stress in the RVLM locally. The overexpression of Mn-SOD in the RVLM caused the sympatho-inhibition, and the depressor and bradycardiac responses were similar to those effects caused by the microinjection of tempol into the RVLM. We consider that microinjection of tempol into the RVLM locally causes the sympatho-inhibition due to the reduction of oxidative stress in the RVLM locally. Furthermore, to increase the oxidative stress in the RVLM, we microinjected angiotensin II into the RVLM of OP, OR, CTR-OP, and CR-OP. Previously, we performed the same experiments in the hypertensive model rats, in which the microinjection of angiotensin II into the RVLM increased sympathetic nerve activity due to the increase in oxidative stress in the RVLM (20).

MATERIALS AND METHODS

Animals

This study was reviewed and approved by the Committee on Ethics of Animal Experiments, Kyushu University Graduate School of Medical Sciences, and conducted according to the Guidelines for Animal Experiments of Kyushu University. Male Sprague-Dawley rats (Charles River Laboratories, Kingston, NY) weighing between 350 to 425 g were housed individually in a temperature-controlled room (22° to 23°C) with a 12-h/12-h light-dark cycle (lights on at 7:00 AM). Rats were placed on a moderate high-fat diet (32% kcal from fat, Research Diets, New Brunswick, NJ) for 13 weeks. After 5 weeks, rats fed the moderately high-fat diet segregate into obesity prone (OP) and obesity resistance (OR) based on the body weight distribution as described previously (23). Briefly, a body weight histogram was constructed and resulted in a distribution of rats into OP and OR groups corresponding with the upper and lower one-third of rats, respectively.

Calorie Restriction

Obesity prone rats in the calorie restriction (CR-OP) group were given 70% of their mean 24-h food intake. Food was given to the CR-OP group daily 2–3 h before lights off. The restricted feeding was continued for 8 weeks (24). Obesity prone rats in the control (CTR-OP) group were free to have food.

Measurement of BP, HR, and SNA

Systolic blood pressure (SBP) and HR were measured using the tail-cuff method (BP-98A; Softron, Tokyo, Japan). We calculated the urinary norepinephrine excretion for 24 h as an indicator of SNA, as described previously (12, 14).

Measurement of TBARS

To obtain the RVLM tissues, the rats were deeply anesthetized with sodium pentobarbital (100 mg/kg IP) and perfused transcardially with PBS (150 mol/L NaCl, 3 mmol/L KCl, and 5 nmol/L phosphate; pH 7.4, 4°C). The brains were removed quickly, and sections 1 mm thick were obtained with a cryostat at -7 ± 1°C. The RVLM was defined according to a rat brain atlas as described previously (12), and obtained by a punch-out technique. The RVLM tissues were homogenized in 1.15% KCl (pH 7.4) and 0.4% sodium dodecyl sulfate, 7.5% acetic acid adjusted to pH 3.5 with NaOH. Thiobarbituric acid (0.3%) was added to the homogenate. The mixture was maintained at 5°C for 60 min, followed by heating to 100°C for 60 min. After cooling, the mixture was extracted with distilled water and *n*-butanolpyridine (15:1) and centrifuged at 1600*g* for 10 min. The absorbance of the organic phase was measured at 532 nm. The amount of thiobarbituric acid-reactive substances (TBARS) was determined by absorbance, as described previously (12).

Microinjection of Tempol and Angiotensin II into the RVLM

To inhibit the oxidative stress in the RVLM, we microinjected tempol (1 nmol) into the RVLM of OP, OR, CTR-OP, and CR-OP which were anesthetized with sodium pentobarbital , as described previously (12). One h after the microinjection of tempol, we determined the recovery of BP and HR to the levels of baseline, and we microinjected angiotensin II (50 pmol) into the RVLM. A catheter was inserted into the femoral artery to record arterial BP. A tracheal cannula was connected to a ventilator, and the rats were artificially ventilated. The rats were placed in a stereotaxic frame. A glass micropipette was filled with tempol, angiotensin II, or L-glutamate and positioned at the injection site. Before the microinjection, the RVLM was identified by monitoring the mean arterial pressure (MAP) after injection of a small dose of L-glutamate. The identification of the RVLM was confirmed as described previously (12).

Statistical Analysis

All values are expressed as mean ± SEM. Comparisons between any two mean values were performed using Bonferroni's correction for multiple comparisons. ANOVA was used to compare the body weight, blood pressure, and TBARS levels in CR-OP or CTR-OP.

Differences were considered to be statistically significant at a P value of <0.05.

RESULTS

Body Weight, BP, HR, Urinary Norepinephrine Excretion, and TBARS levels in the RVLM before CR

Before the start of the CR, OP rats weighed significantly more than OR (Figure 1). Systolic BP and HR were also significantly higher in OP than in OR (Figures 2A and 2B). The peak of the depressor and bradycardiac responses due to the microinjection of tempol into the RVLM was around 10 min after the injection, and the responses were significantly greater in OP than OR (-24 ± 4 mmHg vs. -7 ± 5 mmHg, -30 ± 6 bpm vs. -4 ± 3 bpm, n = 4 for each, P < 0.05 for each, Figure 3A). The peak of the presser and tachycardic responses due to the microinjection of angiotensin II into the RVLM was around 15 min after the injection, and the responses were significantly greater in OP than in OR (Figure 3B). Urinary norepinephrine excretion was significantly higher in OP than in OR (Figure 4A). TBARS levels in the RVLM were significantly higher in OP than in OR (Figure 4B).

Body Weight, BP, HR, Urinary Norepinephrine Excretion, and TBARS levels in the RVLM after CR

Eight weeks after the CR, CR-OP rats weighed significantly less than CTR-OP and OP before CR (Figure 1). Systolic blood pressure and HR were also significantly lower in CR-OP than in CTR-OP and in OP before CR (Figures 2A and 2B). The depressor effects and bradycardia due to the microinjection of tempol into the RVLM were significantly smaller in CR-OP than in CTR-OP (-14 ± 3 mmHg vs. -28 ± 4 mmHg, -11 ± 6 bpm vs. -38 ± 4 bpm, n = 4 for each, P < 0.05 for each, Figure 3A). The pressor effects and tachycardia due to the microinjection of angiotensin II into the RVLM were significantly smaller in CR-OP than in CTR-OP (Figure 3B). Urinary norepinephrine excretion was significantly lower in CR-OP than in CTR-OP and in OP before CR (Figure 4A). TBARS levels in the RVLM were significantly lower in CR-OP than in CTR-OP and in OP before CR (Figure 4B).

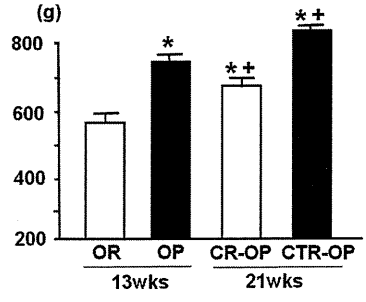

Figure 1. Body weights of OP and OR before calorie restriction, and CR-OP and CTR-OP after calorie restrictions for 8 weeks. Data are shown as mean ± SEM (n = 5 for each group). *P < 0.05 vs. OR; +P < 0.05 vs. OP.

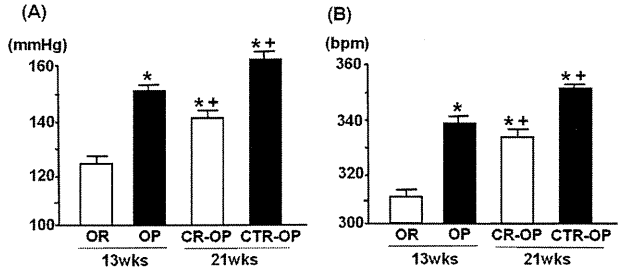

Figure 2. **(A)** Systolic blood pressure of OP and OR before calorie restriction, and CR-OP and CTR-OP after calorie restriction for 8 weeks. Data are shown as mean ± SEM (n =5 for each group). *P < 0.05 vs. OR; +P < 0.05 vs. OP. **(B)** Heart rate of OP and OR before calorie restriction, and CR-OP and CTR-OP after calorie restriction for 8 weeks. Data are shown as mean ± SEM (n = 5 for each group). *P < 0.05 vs. OR; +P < 0.05 vs. OP.

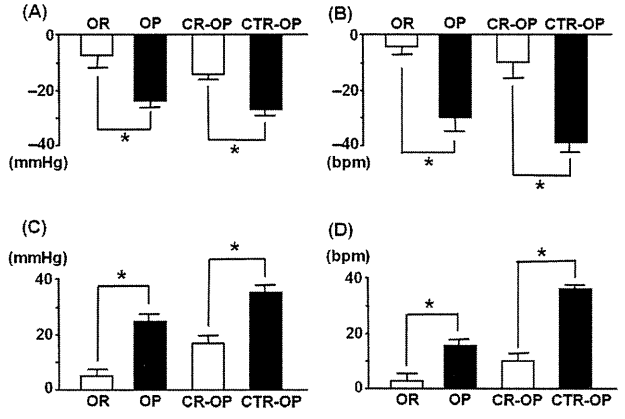

Figure 3. **(A)** Changes in mean BP due to the microinjection of tempol into the RVLM of OP, OR, CR-OP, and CTR-OP. Data are shown as mean ± SEM (n = 4 for each group). *P < 0.05. **(B)** Changes in HR due to the microinjection of tempol into the RVLM of OP, OR, CR-OP, and CTR-OP. Data are shown as mean ± SEM (n = 4 for each group). *P < 0.05. **(C)** Changes in mean BP due to the microinjection of angiotensin II into the RVLM of OP, OR, CR-OP, and CTR-OP. Data are shown as mean ± SEM (n = 4 for each group). *P < 0.05. **(D)** Changes in HR due to the microinjection of angiotensin II into the RVLM of OP, OR, CR-OP, and CTR-OP. Data are shown as mean ± SEM (n = 4 for each group). *P < 0.05.

DISCUSSION

In the present study, we have demonstrated three findings for the first time. First, in obesity-induced hypertensive rats, oxidative stress in the RVLM was increased. Second, calorie restriction decreased sympathetic nerve activity and oxidative stress in obesity-induced hypertensive rats. Third, the depressor and bradycardic response caused by the inhibition of oxidative stress in the RVLM locally were significantly smaller in calorie-restricted obesity rats than in control-obesity rats. These results suggest that obesity enhances oxidative stress in the RVLM, which causes sympatho-excitation and

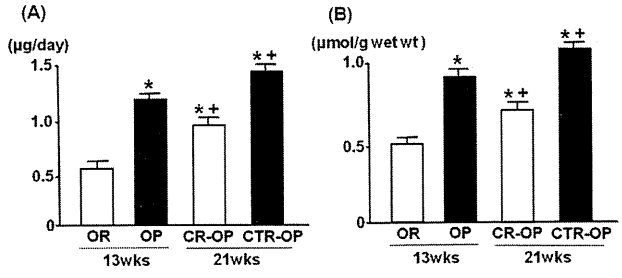

Figure 4. **(A)** Twenty-four hour norepinephrine excretions per body weights of OP and OR before calorie restriction, and CR-OP and CTR-OP after calorie restriction for 8 weeks. Data are shown as mean ± SEM (n = 5 for each group). *P < 0.05 vs. OR; +P < 0.05 vs. OP. **(B)** TBARS levels in the RVLM of OP and OR before calorie restriction, and CR-OP and CTR-OP after calorie restriction for 8 weeks. Data are shown as mean ± SEM (n = 5 for each group). *P < 0.05 vs. OR; +P < 0.05 vs. OP.

hypertension, and that calorie restriction reduces not only body weight but also SNA, probably due to the anti-oxidant in the RVLM.

In the present study, we demonstrated that oxidative stress in the RVLM is increased in obesity-induced hypertensive rat, and that the depressor and bradycardic response caused by the inhibition of oxidative stress in the RVLM locally due to the microinjection of tempol were significantly greater in obesity-induced hypertensive rats than in obesity-resistance rats. Several reports suggest that oxidative stress in the kidney (4), heart (5), and arteries (4, 5) is involved in obesity-induced hypertension. In the brain, high dietary fat has been reported to induce oxidative stress and inflammation in the brain (25), and other previous report have suggested that oxidative stress in the hypothalamus is increased, which cause sympatho-excitation in obesity-induced hypertensive rats (3). Although the RVLM is a vasomotor center and oxidative stress in the RVLM is the most major sympatho-exciting factor, this is the first study examining the oxidative stress in the RVLM of obesity-induced hypertensive rats. However, the mechanisms in which obesity increase oxidative stress in the RVLM have not been conclusive in the present study. Several studies have shown that the central renin-angiotensin system mediates oxidative stress (26, 27), and it is well known that adipose tissue can secrete angiotensinogen (28). In the present study, we demonstrated that the microinjection of angiotensin II into the RVLM caused presser response and tachycardia, and that the effects were significantly greater in OP than in OR, and were significantly smaller in CR-OP than in CTR-OP. Furthermore, rats fed a high fructose diet, a model of insulin resistance, have an increased oxidative stress (29). A peroxisome proliferator-activated receptor-gamma agonist, which ameliorates insulin resistance, prevented hypertension and oxidative stress in dietary-induced obesity rats (30). In addition, there is a possibility that leptin, a polypeptide hormone mediator produced by adipocytes, stimulates oxidative stress generation in the brain (31). We consider that the increase in oxidative stress in the RVLM through the renin-angiotensin system is the most important factor in the obesity-induced hypertension, because oxidative stress in the RVLM is the most major sympatho-exciting factor (12).

Moreover, in the present study, we also demonstrated that calorie restriction inhibits oxidative stress in the RVLM of obesity-induced hypertensive rats, and that the depressor and bradycardic response caused by the inhibition of oxidative stress in the RVLM locally were significantly smaller in calorie-restricted obesity rats than in control-obesity rats. This reduction of oxidative stress in the RVLM might cause sympatho-inhibition. This is the first study which demonstrates that calorie restriction inhibits oxidative stress in the brain.

Although the mechanism in which calorie restriction inhibits oxidative stress in the brain could not been determined in the present study, we hypothesize that calorie restriction may improve adipocytes, inhibit central renin-angiotensin system, directly inhibit oxidative stress in the RVLM, and indirectly inhibit oxidative stress in the RVLM through the inhibition of oxidative stress in the hypothalamus. Circulating angiotensin II acts at circumventricular organs to subsequently activate complex pathways, including those using central angiotensin II as a neurotransmitter, to increases sympathetic outflow (32). However, it is necessary to do further examination.

There are some limitations in the present study. First, we only examined the oxidative stress in the RVLM. There are some important nuclei and areas involved in the cardiovascular control, such as nucleus tractus solitarii, hypothalamus, and so on. The increase in oxidative stress in the obesity-induced hypertension and the reduction of oxidative stress due to calorie restriction may not be the unique phenomenon in the RVLM. From this reason, in the present study, we examined only TBARS methods for the RVLM tissues obtained by the punch-out method, not the histologic examination. However, in the regulation of sympathetic nerve activity, RVLM is the most important cite. Furthermore, in the RVLM, oxidative stress is the most powerful and important sympatho-exciting factor. In the present study, we focused on the oxidative stress in the RVLM of obesity-induced hypertensive rats. Second, in the present study, we could not check the renin-angiotensin system in the RVLM. In the RVLM, oxidative stress is generated by AT_1R and NAD (P) H oxidase. We have the speculation that AT_1R and NAD (P) H oxidase in the RVLM may be activated in the obesity-induced hypertension, and that calorie restriction inhibits AT_1R and NAD (P) H oxidase in the RVLM. We have to perform further studies.

CONCLUSIONS

Our results suggest that, in obesity-induced hypertensive rats, oxidative stress in the RVLM is increased,

and that calorie restriction decreases sympathetic nerve activity through the anti-oxidant in the RVLM of obesity-induced hypertensive rats. These results suggest that obesity enhances oxidative stress in the RVLM, which causes sympatho-excitation and hypertension, and that calorie restriction reduces not only body weight but also sympathetic nerve activity, probably due to the anti-oxidant in the RVLM.

ACKNOWLEDGMENTS

This study was supported by a grant-in-aid for scientific research from the Japan Society for the Promotion of Science (B19390231) and, in part, by the Health and Labor Sciences Research Grant for Comprehensive Research in Aging and Health Labor and Welfare of Japan. We express thanks to Satomi and Jiro.

Declaration of interest: The authors report no conflicts of interest. The authors alone are responsible for the content and writing of the papers.

REFERENCES

[1] Dandona P, Aljada A, Chaudhuri A, Mohanty P, Garg R. Metabolic syndrome: a comprehensive perspective based on interactions betweenobesity, diabetes, and inflammation. *Circulation* 2005;111:1448–1454.

[2] Esler M, Straznicky N, Eikelis N, Masuo K, Lambert G, Lambert E. Mechanisms of sympathetic activation in obesity-related hypertension. *Hypertension* 2006;48:787–796.

[3] Nagae A, Fujita M, Kawarazaki H, Matsui H, Ando K, Fujita T. Sympathoexcitation by oxidative stress in the brain mediates arterial pressure elevation in obesity-induced hypertension. *Circulation* 2009;119:978–986.

[4] Dobrian AD, Davies MJ, Schriver SD, Lauterio TJ, Prewitt RL. Oxidative stress in a rat model of obesity-induced hypertension. *Hypertension* 2001;37:554–560.

[5] Matsui H, Ando K, Kawarazaki H, Nagae A, Fujita M, Shimosawa T, Nagase M, Fujita T. Salt excess causes left ventricular diastolic dysfunction in rats with metabolic disorder. *Hypertension* 2008;52:287–294.

[6] Smith AD, Brands MW, Wang MH, Dorrance AM. Obesity-induced hypertension develops in young rats independently of the renin-angiotensin-aldosterone system. *Exp Biol Med (Maywood)* 2006;231:282–287.

[7] Holloszy JO, Fontana L. Caloric restriction in humans. *Exp Gerontol* 2007;42:709–712.

[8] Pedrozo H, Bertrand HA, Herlihy JT. Caloric restriction alters arterialblood pressure and baroreflex responsiveness of the SHR. *Age* 1994;17:23–27.

[9] Young JB, Mullen D, Landsberg L. Caloric restriction lowers bloodpressure in the SHR. *Metab Clin Exp* 1978;27: 1711–1714.

[10] Dampney RA. Functional organization of central pathways regulating the cardiovascular system. *Physiol Rev* 1994;74: 323–364.

[11] Guyenet PG. The sympathetic control of blood pressure. *Nat Rev Neurosci* 2006;7:335–346.

[12] Kishi T, Hirooka Y, Kimura Y, Ito K, Shimokawa H, Takeshita A. Increased reactive oxygen species in rostral ventrolateral medulla contribute to neural mechanisms of hypertension in stroke-prone spontaneously hypertensive rats. *Circulation* 2004;109:3257–3262.

[13] Kishi T, Hirooka Y, Konno S, Ogawa K, Sunagawa K. Angiotensin II type 1 receptor-activated caspase-3 through ras/mitogen-activated protein kinase/extracellular signal-regulated kinase in the rostral ventrolateral medulla is involved in sympathoexcitation in stroke-prone spontaneously hypertensive rats. *Hypertension* 2010;55:291–297.

[14] Kishi T, Hirooka Y, Sakai K, Shigematsu H, Shimokawa H, Takeshita A. Overexpression of eNOS in the RVLM causes hypotension and bradycardia via GABA release. *Hypertension* 2001;38:896–901.

[15] Hirooka Y, Sakai K, Kishi T, Takeshita A. Adenovirus-mediated gene transfer into the NTS in conscious rats. A new approach to examining the central control of cardiovascular regulation. *Ann N Y Acad Sci* 2001;940:197–205.

[16] Hirooka Y, Kishi T, Sakai K, Shimokawa H, Takeshita A. Effect of overproduction of nitric oxide in the brain stem on the cardiovascular response in conscious rats. *J Cardiovasc Pharmacol* 2003;41:S119–S126.

[17] Hirooka Y, Shigematsu H, Kishi T, Kimura Y, Ueta Y, Takeshita A. Reduced nitric oxide synthase in the brainstem contributes to enhanced sympathetic drive in rats with heart failure. *J Cardiovasc Pharmacol* 2003;42:S111–S115.

[18] Sakai K, Hirooka Y, Shigematsu H, Kishi T, Ito K, Shimokawa H, Takeshita A, Sunagawa K. Overexpression of eNOS in brain stem reduces enhanced sympathetic drive in mice with myocardial infarction. *Am J Physiol* 2005;289:H2159–H2166.

[19] Nozoe M, Hirooka Y, Koga Y, Sagara Y, Kishi T, Engelhardt JF, Sunagawa K. Inhibition of Rac1-derived reactive oxygen species in nucleus tractus solitarius decreases blood pressure and heart rate in stroke-prone spontaneously hypertensive rats. *Hypertension* 2007;50:62–68.

[20] Nozoe M, Hirooka Y, Koga Y, Araki S, Konno S, Kishi T, Ide T, Sunagawa K. Mitochondria-derived reactive oxygen species mediate sympathoexcitation induced by angiotensin II in the rostral ventrolateral medulla. *J Hypertens* 2008;26:2176–2184.

[21] Kishi T, Hirooka Y, Shimokawa H, Takeshita A, Sunagawa K. Atorvastatin reduces oxidative stress in the rostral ventrolateral medulla in stroke-prone spontaneously hypertensive rats. *Clin Exp Hypertens* 2008;30:1–9.

[22] Kishi T, Hirooka Y, Ito K, Sakai K, Shimokawa H, Takeshita A. Cardivascular effects of overexpression of endothelial nitric oxide synthase in the rostral ventrolateral medulla in stroke-prone spontaneously hypertensive rats. *Hypertension* 2002;39:264–268.

[23] Stocker SD, Meador R, Adams JM. Neurons of the rostral ventrolateral medulla contribute to obesity-induced hypertension in rats. *Hypertension* 2007;49:640–646.

[24] Teske JA, Kotz CM. Effect of acute and chronic calonic restriction and metabolic glucoprivation on spontaneous physical activity in obesity-prone and obesity-resistance rats. *Am J Physiol* 2009;297:R176–R184.

[25] Zhang X, Dong X, Ren J, Driscoll MJ, Culver B. High dietary fat induces NADPH oxidase-associated oxidative stress and inflammation in rat cerebral cortex. *Exp Neurol* 2005;191: 318–325.

[26] Zimmerman MC, Lazartigues E, Sharma RV, Davisson RL. Hypertension caused by angiotensin II infusion involves increased superoxide production in the central nervous system. *Circ Res* 2004;95:210–216.

[27] Zimmerman MC, Lazartigues E, Lang JA, Sinnayah P, Ahmad IM, Spitz DR, Davisson RL. Superoxide mediates the actions of angiotensin II inthe central nervous system. *Circ Res* 2002;91:1038–1045.

[28] Boustany CM, Bharadwaj K, Daugherty A, Brown DR, Randall DC, Cassis LA. Activation of the systemic and adipose renin-angiotensin system in rats with diet-induced obesity and hypertension. *Am J Physiol* 2004;287:R943–R949.

[29] Delbosc S, Paizanis E, Magous R, Araiz C, Dimo T, Cristol JP, Cros G, Azay J. Involvement of oxidative stress and NADPH

oxidase activation in the development of cardiovascular complications in a model of insulin resistance, the fructose-fed rat. *Atherosclerosis* 2005;179:43–49.

[30] Dobrian AD, Schriver SD, Khraibi AA, Prewitt RL. Pioglitazone prevents hypertension and reduces oxidative stress in diet-induced obesity. *Hypertension* 2004;43:48–56.

[31] Lauterio TJ, Davies MJ, DeAngelo M, Peyser M, Lee J. Neuropeptide Y expression and endogenous leptin concentrations in a dietary model of obesity. *Obes Res* 1999;7:498–505.

[32] Ferguson AV, Washburn DL. Angiotensin II: a peptidergic neurotransmitter in central autonomic pathways. *Prog Neurobiol* 1998;54:169–192.

Clinical and Experimental Hypertension, 33(4):223–230, (2011)

ISSN 1064-1963 print/1525-6006 online
DOI: 10.3109/10641963.2011.583967

informa
healthcare

Role of Angiotensin-(1-7) in Rostral Ventrolateral Medulla in Blood Pressure Regulation via Sympathetic Nerve Activity in Wistar-Kyoto and Spontaneous Hypertensive Rats

Toshiaki Nakagaki,[1,2] Yoshitaka Hirooka,[1] Koji Ito,[1] Takuya Kishi,[1] Sumio Hoka,[2] Kenji Sunagawa[1]

[1]*Department of Cardiovascular Medicine, Kyushu University Graduate School of Medical Sciences, Fukuoka, Japan,*
[2]*Department of Anesthesiology and Critical Care Medicine, Kyushu University Graduate School of Medical Sciences, Fukuoka, Japan*

Abstract

Angiotensin (Ang)-(1-7) Ang-(1-7) is formed from angiotensin II by angiotensin-converting enzyme 2 (ACE2) and modulates the renin-angiotensin system. We evaluated whether the Ang-(1-7)-Mas axis in the rostral ventrolateral medulla (RVLM) contributes to neural mechanisms of blood pressure (BP) regulation. We microinjected Ang-(1-7), Ang-(1-7)-Mas receptor antagonist A-779, and ACE2 inhibitor DX600 into the RVLM of anesthetized Wistar-Kyoto rats (WKY) and spontaneously hypertensive rats (SHRs). Unilateral Ang-(1-7) microinjection induced a significantly greater increase in AP (arterial blood pressure) in SHR than in WKY. Bilateral A-779 microinjection induced a significantly greater decrease in AP and renal sympathetic nerve activity in SHR than in WKY. Bilateral DX600 microinjection induced a significantly greater decrease in AP in SHR than in WKY. Our results suggest that endogenous Ang-(1-7) in the RVLM contributes to maintain AP and renal sympathetic nerve activity both in SHR and WKY and that its activity might be enhanced in SHR.

keywords: angiotensin-(1-7), blood pressure, sympathetic nervous system, rostral ventrolateral medulla, hypertension

INTRODUCTION

Accumulating evidence indicates that the sympathetic nervous system plays an important role in the pathogenesis of hypertension (1–3). It is well established that the renin-angiotensin system (RAS) modulates blood pressure (BP) (4). The RAS members may act as neuromodulators in different sites of the brain, and dysfunction in the brain RAS is implicated in the pathogenesis of hypertension (5). The rostral ventrolateral medulla (RVLM) is the major vasomotor center that determines basal sympathetic nervous system activity and is essential for the maintenance of basal vasomotor tone (6). Activation of angiotensin type 1 (AT_1) receptors in the RVLM evokes sympathetic excitation and pressor effects in normal animals (7,8) and appears to be important for the maintenance of hypertension in spontaneously hypertensive rats (SHR) (9).

Angiotensin-(1-7) [Ang-(1-7)] is a biologically active peptide of the RAS family. It is formed from angiotensin (Ang) I or II by an angiotensin-converting enzyme homolog (ACE2) (10). The action of Ang-(1-7) is mediated through its selective receptor Mas (11), which is different from AT_1 or AT_2 receptor subtypes, and is blocked by its specific antagonist A-779. Ang-(1-7) is active in central areas of cardiovascular control, including neurons in the nucleus tractus solitarius (NTS) (12), RVLM (13,14), and paraventricular nucleus (PVN) (15). The Mas receptor and ACE2 are present in different areas related to cardiovascular control in the brain (16,17). Although Ang II and Ang-(1-7) have opposite effects systemically, microinjection of Ang-(1-7) or Ang-II into the RVLM elicits a similar pressor response (18,19).

The objective of the present study was to determine whether Ang-(1-7) in the RVLM contributes to the maintenance or elevation of BP in a rat model of hypertension. Therefore, we investigated the cardiovascular effects of microinjection of Ang-(1-7), its selective antagonist A-779, and the ACE2 inhibitor DX600 into the RVLM in normotensive and hypertensive rats.

Address correspondence to Yoshitaka Hirooka, MD, PhD, FAHA, Department of Cardiovascular Medicine, Kyushu University Graduate School of Medical Sciences, 3-1-1 Maidashi, Higashi-ku, Fukuoka, 812-8582, Japan. E-mail: hyoshi@cardiol.med.kyushu-u.ac.jp
Received 30 August 2010; revised 13 October 2010; accepted 27 October 2010.

METHODS

This study was reviewed and approved by the Committee of Ethics of Animal Experiments, Kyushu University Graduate School of Medical Sciences, and was conducted according to the Guidelines for Animal Experiments of Kyushu University.

Animals and General Procedures

Male Wistar-Kyoto/Izm rats (WKY) and spontaneously hypertensive/Izm rats (SHRs) (12–16 weeks old, SLC Japan, Hamamatsu, Japan) were used. Food and tap water were available *ad libitum* throughout the study. The rats were kept in a temperature- and humidity-controlled room under a 12-h light period between 8:00 AM and 8:00 PM. To obtain RVLM tissues, the rats were deeply anesthetized with sodium pentobarbital (100 mg/kg i.p.) and transcardially perfused with phosphate-buffered saline (150 mol/L NaCl, 3 mmol/L KCl, and 5 nmol/L phosphate; pH 7.4, 4°C). The brains were quickly removed, and 1-mm thick sections were obtained with a cryostat at −7±1°C. The RVLM was defined according to a rat brain atlas and the RVLM tissue was obtained using a punch-out technique, as previously described (6).

Microinjection into the RVLM

Spontaneously hypertensive rats and WKYs were initially anesthetized with sodium pentobarbital (50 mg/kg i.p., followed by a maintenance dosage of 20 mg/kg/h i.v.). A catheter was inserted into the femoral artery to record arterial blood pressure (AP) and heart rate (HR). A tracheal cannula was connected to a ventilator, and the rats were artificially ventilated. Body temperature was monitored with a rectal thermometer and maintained in the range of 36.5 to 37.5°C with a heating pad. The left kidney was exposed using a retroperitoneal approach, and the renal nerve prepared for recording renal sympathetic nerve activity (RSNA) as previously described (20). The rats were placed in a stereotaxic frame with the incisor bar and the dorsal surface of the medulla was surgically exposed to allow for positioning of the microinjection pipettes into the RVLM (with the pipette angled rostrally 18°, 1.8 mm lateral, 3.5 mm below the calamus scriptorius), as previously described (21). Microinjections (all microinjections were in a volume of 100 nL unless otherwise indicated) into the RVLM were made according to the following protocols: (1) unilateral microinjection of Ang-(1-7) (100 pmol); (2) bilateral microinjections of A-779 (100 pmol each); (3) unilateral microinjection of Ang-(1-7) (100 pmol each) 30 min after bilateral injections of A-779 (100 pmol each); (4) unilateral microinjection of Ang-(1-7) (100 pmol) 15 min after bilateral injections of AT_1 receptor antagonist valsartan (100 pmol each); (5) bilateral microinjection of ACE2 inhibitor DX600 (25 pmol in 50 nL each). Ang-(1-7) and A-779 were obtained from Bachem Inc. (Bubendorf, Switzerland). DX600 was obtained from Phoenix Pharmaceuticals (Burlingame, CA). The AT_1 receptor antagonist valsartan was a gift from Novartis Pharma AG (Basel, Switzerland). Drug doses were based on previous reports (9,15,19) or on preliminary experiments. Before microinjection of the drugs, the RVLM was identified by monitoring the mean arterial pressure (MAP) after injecting a small dose of L-glutamate. For bilateral injections, injections were first made on one side, and then the pipette was moved to the contralateral side; the two injections were made ~3 min apart. To verify the injection site histologically, 50 nL of Evans Blue dye was injected into the site at the end of the microinjection experiments. The rats were deeply anesthetized with an excessive dose of sodium pentobarbital, and transcardially perfused with 4% paraformaldehyde in phosphate-buffered saline. The brain was removed and sectioned to verify the microinjection sites. The rats whose microinjection sites were within the boundaries of the RVLM were used for data analysis.

Western Blot Analysis of the Mas Receptor in the RVLM

The RVLM tissue was homogenized and then sonicated in lysing buffer containing 40 mmol/L 4-(2-hydroxyethyl)-1-piperazineethanesulfonic acid (HEP ES), 1% Triton X-100, 10% glycerol, 1 mmol/L phenylmethanesulfonyl fluoride, and 1 mmol/L protease inhibitor cocktail tablet (Roche Diagnostics, Indianapolis, IN). The tissue lysate was centrifuged at 6000 rpm for 5 min at 4°C in a microcentrifuge. The lysate was collected and the protein concentration was determined using a bincinchoninic acid protein assay kit (Pierce, Rockford, IL). Aliquots of protein (50 μg) from each sample were separated on a 7.5% sodium dodecyl sulfate-polyacrylamide gel. Subsequently, the separated proteins were transferred onto polyvinylidene difluoride membranes (Immobilon-P membrane; Millipore, Billerica, MA). The membranes were incubated with goat IgG polyclonal antibody against Mas (1:1000; Santa Cruz Biotechnology, Santa Cruz, CA) and with rabbit IgG polyclonal antibody against GAPDH (1:1000; Santa Cruz Biotechnology) for 24 to 48 h. The membranes were then washed and incubated with horseradish peroxidase-conjugated horse anti-goat IgG or anti-rabbit antibody (1:10000; Santa Cruz Biotechnology) for 40 min. Immunoreactivity was detected by autoradiography using enhanced chemiluminescence and a western blotting detection kit (Amersham, Piscataway, NJ).

Statistical Analysis

All values are expressed as means ± SEM. The changes in MAP, HR, and RSNA values during the microinjection study were compared using a unpaired *t*-test or analysis of variance where appropriate. A P value of less than 0.05 was considered statistically significant.

RESULTS

Microinjection of Ang-(1-7) or A-779 into the RVLM

Unilateral microinjection of Ang-(1-7) into the RVLM increased AP in both strains, but the increase was significantly greater in SHR than in WKY ($P < 0.05$; Figures 1A and 1B). No significant changes in HR were observed in either strain. In contrast, bilateral microinjection of A-779 into the RVLM induced a significant decrease in AP and RSNA in both strains. The decreases in AP and RSNA were significantly greater in SHR than in WKY ($P < 0.05$; Figures 2A and 2B).

Effect of Valsartan or A-779 on the Ang-(1-7)-Induced Responses

Pretreatment with bilateral microinjection of A-779 into the RVLM attenuated the Ang-(1-7)-induced increase in AP (Figure 3A). Valsartan pretreatment did not change the Ang-(1-7)-induced increase in AP (Figure 3B).

Mas Receptor Expression in the RVLM

Mas receptor expression levels in the RVLM were significantly higher in SHR than in WKY ($P < 0.05$; Figure 4).

Microinjection of ACE2 Inhibitor DX600 into the RVLM

Bilateral microinjection of the ACE2 inhibitor, DX600, in the RVLM induced a significant decrease in AP in both strains. The decrease in AP was significantly greater in SHR than in WKY ($P < 0.05$; Figure 5).

DISCUSSION

The major findings of the present study were as follows: 1) the blockade of endogenous Ang-(1-7) in the RVLM

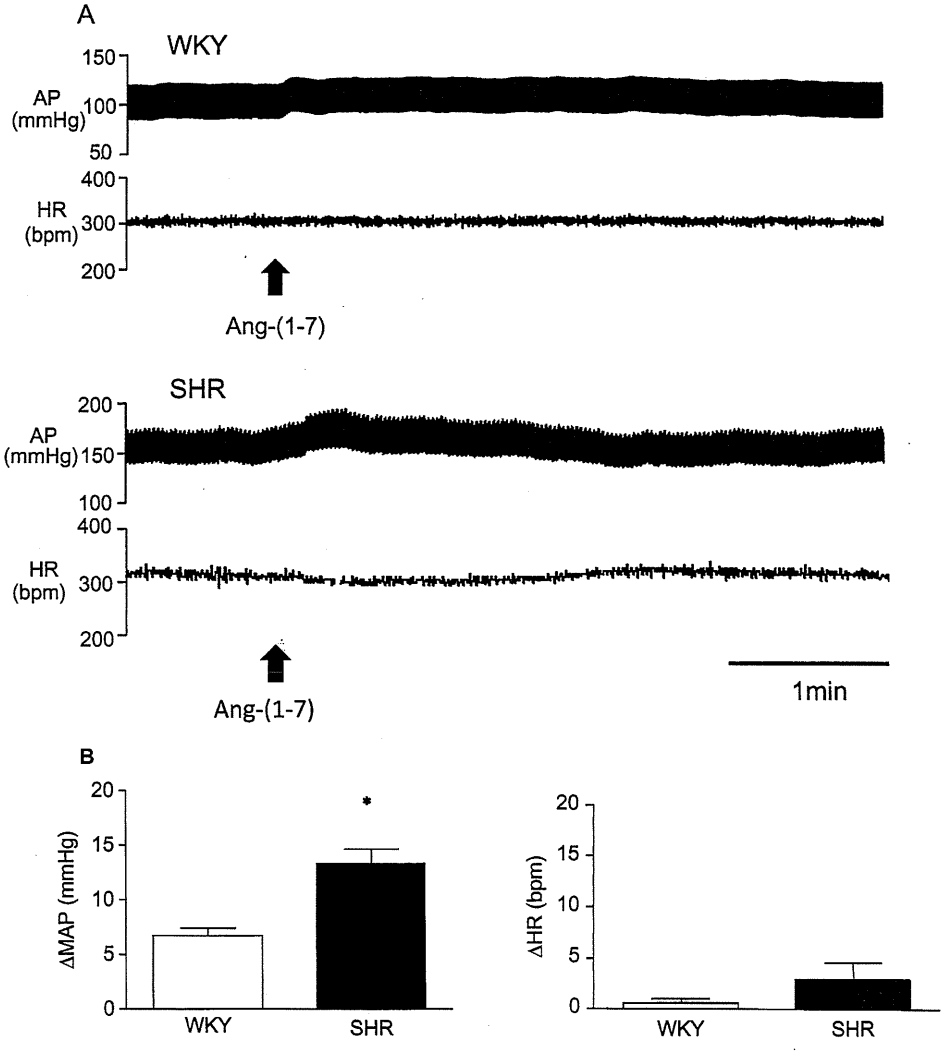

Figure 1. Effect of microinjection of Ang-(1-7) on arterial blood pressure (AP) and heart rate (HR). **A,** Changes in AP and HR after unilateral injection of Ang-(1-7) (100 pmol) into the rostral ventrolateral medulla (RVLM) in Wistar-Kyoto rats (WKY) (top) and spontaneously hypertensive rats (SHR) (bottom) rats. Arrow indicates the time at which Ang-(1-7) was injected. **B,** Grouped data of mean (+ SEM) change from baseline of AP (MAP) and HR evoked by unilateral microinjection of Ang-(1-7) into the RVLM. n = 6 per group. *$P < 0.05$ compared to WKY rats.

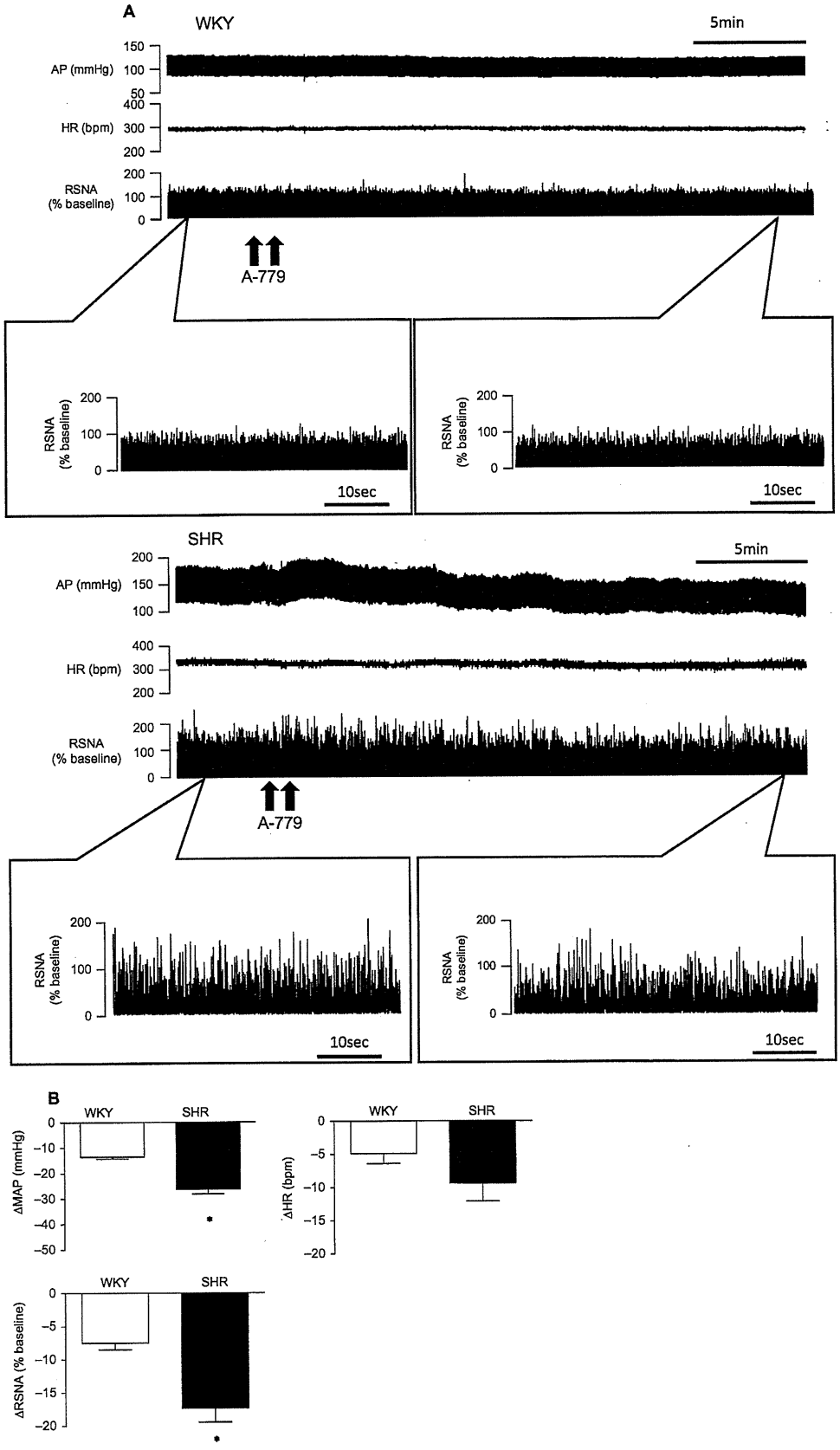

Figure 2. Effect of bilateral microinjection of A-779 on AP, HR, and renal sympathetic nerve activity (RSNA). **A,** Original recording form WKY (top) and SHR (bottom) rats showing AP, HR, and RSNA in response to bilateral microinjection of A-779 (100 pmol) into the RVLM. Arrows indicate the time at which A-779 was injected. **B,** Grouped data of mean (+ SEM) change from baseline of MAP, HR, and RSNA evoked by bilateral microinjection of A-779 into the RVLM. n = 5 per group. *P < 0.05 compared to WKY rats.

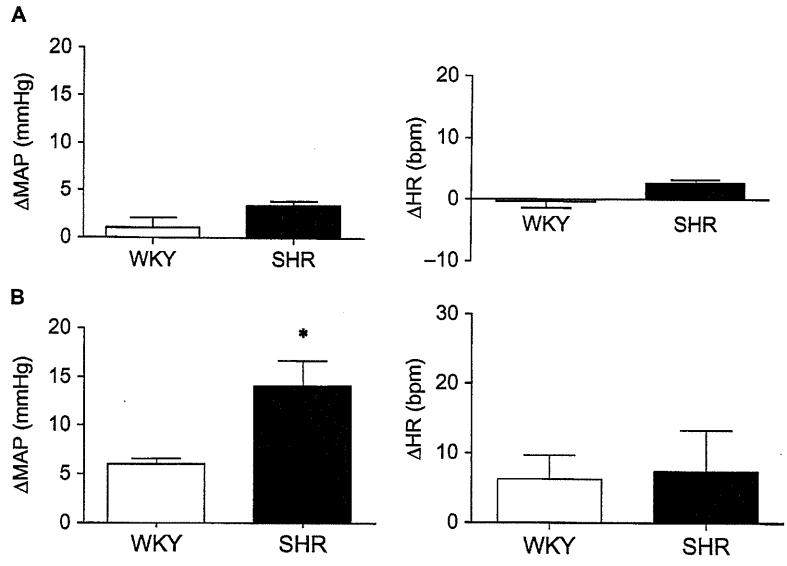

Figure 3. The effect of the microinjection of Ang-(1-7) into the RVLM pretreated with angiotensin antagonists. **A,** Group data of the mean (+SEM) change in MAP and HR in response to microinjection of Ang-(1-7) (100 pmol) pretreated with A-779 (100 pmol). **B,** Group data of the mean (+SEM) change in MAP and HR in response to microinjection with Ang-(1-7) (100 pmol) pretreated valsartan (100 pmol). n = 5 per group. *P < 0.05 compared to WKY rats.

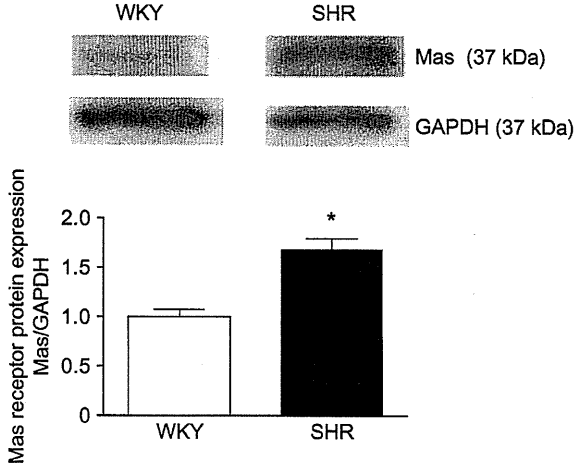

Figure 4. Western blot analysis demonstrating Mas receptor expression in the RVLM. Data are expressed as the ratio relative to GAPDH levels. n= 4 per group. *P < 0.05 compared to WKY rats.

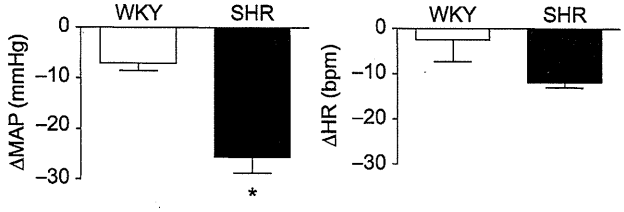

Figure 5. The effect of bilateral microinjection of ACE2 inhibitor DX600 on AP and HR. Grouped data of mean (+SEM) change in MAP and HR evoked by bilateral microinjection of DX600 (25 pmol) into the RVLM. n = 5 per group. *P < 0.05 compared with WKY rats.

significantly decreased AP and RSNA in both WKY and SHR, but the decrease was greater in SHR than in WKY; 2) microinjection of Ang-(1-7) into the RVLM increased AP, and this effect was blocked by the selective Ang-(1-7) antagonist A-779, but not by the AT_1 receptor blocker valsartan; and 3) Mas receptor expression levels in the RVLM were greater in SHRs than in WKYs. Together, these results suggest that endogenous Ang-(1-7) in the RVLM contributes to the maintenance of AP and its activity might be enhanced in SHR compared to WKY.

Our observations are consistent with previous reports that microinjection of Ang-(1-7) into the RVLM increases AP (18,22). Electrophysiological studies demonstrated that most neurons in the PVN are excited by Ang-(1-7) (23), and the Ang-(1-7)-induced firing rate increase of PVN neurons is blocked by A-779 (24). Paraventricular nucleus neurons have excitatory efferents to the RVLM (23, 24). Thus, endogenous Ang-(1-7) likely has a stimulatory effect on RVLM neurons.

Microinjection of AT_1 receptor antagonists into the RVLM decreases AP in SHR but not in control WKY (9,25), suggesting that AT_1 receptors in the RVLM are not activated under baseline conditions in normotensive rats, but AT_1 receptors in the RVLM are tonically stimulated and act to support sympathetic vasomotor tone under basal conditions in SHR. Microinjection of the Ang-(1-7) antagonist A-779 into the RVLM, however, decreased AP in both strains, and the hypotensive effect was greater in SHR than in WKY. These data suggest that the RVLM neurons are tonically stimulated by

endogenous Ang-(1-7) in normal conditions and their stimulation is augmented in SHR.

In the present study, the effect of Ang-(1-7) in the RVLM was not mediated by the AT_1 receptor, but was mediated by the Mas receptor. Previous studies also showed that Ang-(1-7) is an endogenous ligand of the orphan G-protein coupled receptor Mas (11). In fact, the binding of Ang-(1-7) in the kidney and the antidiuretic action of Ang-(1-7) are completely abolished in Mas-knockout mice (11) and Ang-(1-7) also does not induce relaxation in the aorta of Mas-knockout mice (11). These data indicate that Mas is a functional receptor that mediates the physiological actions of Ang-(1-7).

Ang-(1-7) acts as a counterregulatory modulator of Ang II in the central nervous system (4).While Ang II reduces the baroreflex sensitivity (26), Ang-(1-7) facilitates the baroreflex after either intracerebroventricular infusion (27,28) or microinjection into the NTS (29,30), but does not alter the baroreflex after microinjection into the RVLM (31). In the present study, we did not investigate the effect of Ang-(1-7) on baroreflex sensitivity.

The observations that exogenous stimulation of Mas receptors elicits a greater increase in AP and blockade of Mas receptors induces a greater decrease in AP in SHR might relate to an increase in the number of receptors in the RVLM of SHR. Mas receptor protein expression in the RVLM was significantly higher in SHR than in WKY. These findings suggest that activation of the Ang-(1-7)-Mas pathway in the RVLM contributes to the maintenance and increase in AP in SHR.

Recently, ACE2 was identified as a new member of the ACE family (32). This carboxypeptidase cleaves Ang I and Ang II to form Ang-(1-9) and Ang-(1-7), respectively (10,33). ACE2 has an approximately 400-fold greater affinity for Ang II than for Ang I (33). Accordingly, the major role of ACE2 in angiotensin peptide metabolism is the production of Ang-(1-7). In the present study, microinjection of the ACE2 inhibitor DX600 into the RVLM induced a significant decrease in AP in both SHR and WKY, although the decrease in AP was significantly greater in SHR than in WKY. Therefore, we suggest that DX600 into the RVLM might also decrease RSNA as A-779, although we did not measure RSNA directly in the case of DX600. Microinjection of either Ang II or Ang-(1-7) into the RVLM or NTS increases or decreases AP, respectively (18,29). Injection of the ACE2 inhibitor MLN4760 into the NTS decreases AP in normotensive Sprague Dawley rats (34), and in the present study, microinjection of the ACE2 inhibitor DX600 into the RVLM induced a decrease in AP. Injecting an ACE2 inhibitor into the RVLM should decrease Ang-(1-7) levels, providing a potential mechanism for the AP response, although Ang II levels may also increase.

Ang-(1-7) is also formed by the endopeptidase neprilysin from Ang-I or Ang-(1–9) (35). Neprilysin mRNA in the medulla is lower in older rats compared to younger rats, whereas ACE2 and Mas receptor mRNA levels of older rats do not differ from those in younger rats (36). Thus, functional studies are necessary to confirm the altered expression or activity of neprilysin in WKY and SHR. ACE2 might also be involved in the metabolism of other peptides that are not related to RAS, such as apelin, neurotensin, and dynorphin (33,37). Microinjection of neurotensin and apelin into the RVLM increase AP (38,39). Apelin expression is enhanced in the RVLM in SHR compared to WKY (40); thus it is possible that the effect of apelin in the RVLM is also altered in SHR.

Although Ang-(1-7) is reported to play an important role in counteracting the pressor and proliferative actions of Ang II in the heart or vasculature (41,42), in the present study Ang-(1-7) had effects that were similar to those of Ang II in the RVLM. It is not clear why the systemic and central effects of Ang-(1-7) and Ang II are different; Ang-(1-7) may have a distinct mechanism of action in neuronal nuclei such as the RVLM. In addition, the precise mechanism(s) involved in the differences in BP regulation induced by endogenous Ang-(1-7) in the RVLM between SHR and WKY is uncertain because we did not measure endogenous Ang-(1-7) activity directly or Ang-(1-7) concentration in the RVLM.

In conclusion, the findings from the present study suggest that endogenous Ang-(1-7) in the RVLM contributes to tonic maintenance of AP via the sympathetic nervous system both in WKY and SHR and that its activity in Ang-(1-7)-Mas receptor axis might be enhanced in SHR.

ACKNOWLEDGMENTS

This study was supported by a grant-in-aid for scientific research from the Japan Society for the Promotion of Science (B19390231), and in part, by a Health and Labor Sciences Research Grant of Japan. We express our sincere thanks to Naomi Shiouze for help with the western blot analysis.

Declaration of interest: The authors report no conflicts of interest. The authors alone are responsible for the content and writing of the paper.

REFERENCES

[1] Grassi G. Assessment of sympathetic cardiovascular drive in human hypertension: Achievements and perspectives. *Hypertension* 2009;54:690–697.

[2] Esler M. The 2009 Carl Ludwig Lecture: Pathophysiology of the human sympathetic nervous system in cardiovascular diseases: The transition from mechanisms to medical management. *J Appl Physiol* 2010;108:227–237.

[3] Guyenet PG. The sympathetic control of blood pressure. *Nat Rev Neurosci* 2006;7:335–346.
[4] Xia H, Lazartigues E. Angiotensin-converting enzyme 2 in the brain: Properties and future directions. *J Neurochem* 2008;107:1482–1494.
[5] Veerasingham SJ, Raizada MK. Brain renin-angiotensin system dysfunction in hypertension: Recent advances and perspectives. *Br J Pharmacol* 2003;139:191–202.
[6] Kishi T, Hirooka Y, Kimura Y, Ito K, Shimokawa H, Takeshita A. Increased reactive oxygen species in rostral ventrolateral medulla contribute to neural mechanisms of hypertension in stroke-prone spontaneously hypertensive rats. *Circulation* 2004;109:2357–2362.
[7] Fontes MA, Martins Pinge MC, Naves V, Campagnole-Santos MJ, Lopes OU, Khosla MC, Santos RA. Cardiovascular effects produced by microinjection of angiotensins and angiotensin antagonists into the ventrolateral medulla of freely moving rats. *Brain Res* 1997;750:305–310.
[8] Tagawa T, Fontes MA, Potts PD, Allen AM, Dampney RA. The physiological role of AT1 receptors in the ventrolateral medulla. *Braz J Med Biol Res* 2000;33:643–652.
[9] Ito S, Komatsu K, Tsukamoto K, Kanmatsuse K, Sved AF. Ventrolateral medulla AT_1 receptors support blood pressure in hypertensive rats. *Hypertension* 2002;40:552–559.
[10] Tipnis SR, Hooper NM, Hyde R, Karran E, Christie G, Turner AJ. A human homolog of angiotensin-converting enzyme. cloning and functional expression as a captopril-insensitive carboxypeptidase. *J Biol Chem* 2000;275:33238–33243.
[11] Santos RA, Simoes e Silva AC, Maric C, Silva DM, Machado RP, de Buhr I, Heringer-Walther S, Pinheiro SV, Lopes MT, Bader M, Mendes EP, Lemos VS, Campagnole-Santos MJ, Schultheiss HP, Speth R, Walther T. Angiotensin-(1-7) is an endogenous ligand for the G protein-coupled receptor mas. *Proc Natl Acad Sci U S A* 2003;100:8258–8263.
[12] Campagnole-Santos MJ, Diz DI, Santos RA, Khosla MC, Brosnihan KB, Ferrario CM. Cardiovascular effects of angiotensin-(1-7) injected into the dorsal medulla of rats. *Am J Physiol* 1989; 257:H324–H329.
[13] Silva LC, Fontes MA, Campagnole-Santos MJ, Khosla MC, Campos RR Jr, Guertzenstein PG, Santos RA. Cardiovascular effects produced by micro-injection of angiotensin-(1-7) on vasopressor and vasodepressor sites of the ventrolateral medulla. *Brain Res* 1993;613:321–325.
[14] Fontes MA, Baltatu O, Caligiorne SM, Campagnole-Santos MJ, Ganten D, Bader M, Santos RA. Angiotensin peptides acting at rostral ventrolateral medulla contribute to hypertension of TGR(mREN2)27 rats. *Physiol Genomics* 2000;2: 137–142.
[15] Silva AQ, Santos RA, Fontes MA. Blockade of endogenous angiotensin-(1-7) in the hypothalamic paraventricular nucleus reduces renal sympathetic tone. *Hypertension* 2005;46: 341–348.
[16] Doobay MF, Talman LS, Obr TD, Tian X, Davisson RL, Lazartigues E. Differential expression of neuronal ACE2 in transgenic mice with overexpression of the brain renin-angiotensin system. *Am J Physiol Regul Integr Comp Physiol* 2007;292:R373–R381.
[17] Becker LK, Etelvino GM, Walther T, Santos RA, Campagnole-Santos MJ. Immunofluorescence localization of the receptor mas in cardiovascular-related areas of the rat brain. *Am J Physiol Heart Circ Physiol* 2007;293:H1416–H1424.
[18] Fontes MA, Silva LC, Campagnole-Santos MJ, Khosla MC, Guertzenstein PG, Santos RA. Evidence that angiotensin-(1-7) plays a role in the central control of blood pressure at the ventro-lateral medulla acting through specific receptors. *Brain Res* 1994;665:175–180.
[19] Zhou LM, Shi Z, Gao J, Han Y, Yuan N, Gao XY, Zhu GQ. Angiotensin-(1-7) and angiotension II in the rostral ventrolateral medulla modulate the cardiac sympathetic afferent reflex and sympathetic activity in rats. *Pflugers Arch* 2010;459: 681–688.
[20] Ito K, Hirooka Y, Sakai K, Kishi T, Kaibuchi K, Shimokawa H, Takeshita A. Rho/Rho-kinase pathway in brain stem contributes to blood pressure regulation via sympathetic nervous system: Possible involvement in neural mechanisms of hypertension. *Circ Res* 2003;92:1337–1343.
[21] Koga Y, Hirooka Y, Araki S, Nozoe M, Kishi T, Sunagawa K. High salt intake enhances blood pressure increase during development of hypertension via oxidative stress in rostral ventrolateral medulla of spontaneously hypertensive rats. *Hypertens Res* 2008;31:2075–2083.
[22] Santos RA, Campagnole-Santos MJ, Baracho NCV, Fontes MAP, Silva LCS, Neves LAA, Oliveira DR, Caligiorne SM, Rodrigues AR, Gropen C Jr, Carvalho WS, Simoes e Silva AC, Khosla MC. Characterization of a new angiotensin antagonist selective for angiotensin-(1-7): Evidence that the actions of angiotensin-(1-7) are mediated by specific angiotensin receptors. *Brain Res Bull* 1994;35:293–298.
[23] Felix D, Khosla MC, Barnes KL, Imboden H, Montani B, Ferrario CM. Neurophysiological responses to angiotensin-(1-7). *Hypertension* 1991;17:1111–1114.
[24] Ambuhl P, Felix D, Khosla MC. 7-D-ALA]-angiotensin-(1-7): Selective antagonism of angiotensin-(1-7) in the rat paraventricular nucleus. *Brain Res Bull* 1994;35:289–291.
[25] Potts PD, Allen AM, Horiuchi J, Dampney RA. Does angiotensin II have a significant tonic action on cardiovascular neurons in the rostral and caudal VLM? *Am J Physiol Regul Integr Comp Physiol* 2000;279:R1392–R1402.
[26] Casto R, Phillips MI. Angiotensin II attenuates baroreflexes at nucleus tractus solitarius of rats. *Am J Physiol* 1986;250: R193–R198.
[27] Britto RR, Santos RA, Fagundes-Moura CR, Khosla MC, Campagnole-Santos MJ. Role of angiotensin-(1-7) in the modulation of the baroreflex in renovascular hypertensive rats. *Hypertension* 1997;30:549–556.
[28] Oliveira DR, Santos RA, Santos GF, Khosla M, Campagnole-Santos MJ. Changes in the baroreflex control of heart rate produced by central infusion of selective angiotensin antagonists in hypertensive rats. *Hypertension* 1996;27:1284–1290.
[29] Chaves GZ, Caligiorne SM, Santos RA, Khosla MC, Campagnole-Santos MJ. Modulation of the baroreflex control of heart rate by angiotensin-(1-7) at the nucleus tractus solitarii of normotensive and spontaneously hypertensive rats. *J Hypertens* 2000;18:1841–1848.
[30] Couto AS, Baltatu O, Santos RA, Ganten D, Bader M, Campagnole-Santos MJ. Differential effects of angiotensin II and angiotensin-(1-7) at the nucleus tractus solitarii of transgenic rats with low brain angiotensinogen. *J Hypertens* 2002;20:919–925.
[31] Alzamora AC, Santos RA, Campagnole-Santos MJ. Baroreflex modulation by angiotensins at the rat rostral and caudal ventrolateral medulla. *Am J Physiol Regul Integr Comp Physiol* 2006;290:R1027–R1034.
[32] Donoghue M, Hsieh F, Baronas E, Godbout K, Gosselin M, Stagliano N, Donovan M, Woolf B, Robison K, Jeyaseelan R, Breitbart RE, Acton S. A novel angiotensin-converting enzyme-related carboxypeptidase (ACE2) converts angiotensin I to angiotensin 1-9. *Circ Res* 2000;87:E1–E9.
[33] Vickers C, Hales P, Kaushik V, Dick L, Gavin J, Tang J, Godbout K, Parsons T, Baronas E, Hsieh F, Acton S, Patane M, Nichols A, Tummino P. Hydrolysis of biological peptides by human angiotensin-converting enzyme-related carboxypeptidase. *J Biol Chem* 2002;277:14838–14843.
[34] Diz DI, Garcia-Espinosa MA, Gegick S, Tommasi EN, Ferrario CM, Ann Tallant E, Chappell MC, Gallagher PE. Injections of angiotensin-converting enzyme 2 inhibitor MLN4760 into nucleus tractus solitarii reduce baroreceptor reflex sensitivity for heart rate control in rats. *Exp Physiol* 2008;93:694–700.

[35] Rice GI, Thomas DA, Grant PJ, Turner AJ, Hooper NM. Evaluation of angiotensin-converting enzyme (ACE), its homologue ACE2 and neprilysin in angiotensin peptide metabolism. *Biochem J* 2004;383:45–51.

[36] Sakima A, Averill DB, Gallagher PE, Kasper SO, Tommasi EN, Ferrario CM, Diz DI. Impaired heart rate baroreflex in older rats: Role of endogenous angiotensin-(1-7) at the nucleus tractus solitarii. *Hypertension* 2005;46:333–340.

[37] Warner FJ, Smith AI, Hooper NM, Turner AJ. Angiotensin-converting enzyme-2: A molecular and cellular perspective. *Cell Mol Life Sci* 2004;61:2704–2713.

[38] Ishizuka T, Wei X, Kubo T. Cardiovascular effects of microinjections of thyrotropin-releasing hormone, oxytocin and other neuropeptides into the rostral ventrolateral medulla of the rat. *Arch Int Pharmacodyn Ther* 1993;322:35–44.

[39] Seyedabadi M, Goodchild AK, Pilowsky PM. Site-specific effects of apelin-13 in the rat medulla oblongata on arterial pressure and respiration. *Auton Neurosci* 2002;101:32–38.

[40] Zhang Q, Yao F, Raizada MK, O'Rourke ST, Sun C. Apelin gene transfer into the rostral ventrolateral medulla induces chronic blood pressure elevation in normotensive rats. *Circ Res* 2009;104:1421–1428.

[41] Averill DB, Ishiyama Y, Chappell MC, Ferrario CM. Cardiac angiotensin-(1-7) in ischemic cardiomyopathy. *Circulation* 2003;108:2141–2146.

[42] Xu P, Costa-Goncalves AC, Todiras M, Rabelo LA, Sampaio WO, Moura MM, Santos SS, Luft FC, Bader M, Gross V, Alenina N, Santos RA. Endothelial dysfunction and elevated blood pressure in MAS gene-deleted mice. *Hypertension* 2008;51:574–580.

Cardiovascular Research
doi:10.1093/cvr/cvr108

Inhibition of MDM2 attenuates neointimal hyperplasia via suppression of vascular proliferation and inflammation

Toru Hashimoto[1], Toshihiro Ichiki[1,2]*, Jiro Ikeda[1], Eriko Narabayashi[1], Hirohide Matsuura[1], Ryohei Miyazaki[1], Keita Inanaga, Kotaro Takeda[1,2], and Kenji Sunagawa[1]

[1]Department of Cardiovascular Medicine, Kyushu University Graduate School of Medical Sciences, Fukuoka, Japan; and [2]Department of Advanced Therapeutics for Cardiovascular Diseases, Kyushu University Graduate School of Medical Sciences, Fukuoka, Japan

Received 26 August 2010; revised 16 March 2011; accepted 8 April 2011

Time for primary review: 43 days

Aims Tumour protein p53 plays an important role in the vascular remodelling process as well as in oncogenesis. p53 is negatively regulated by murine double minute 2 (MDM2). A recently developed MDM2 inhibitor, nutlin-3, is a non-genotoxic activator of the p53 pathway. So far, the effect of MDM2 inhibition on vascular remodelling has not been elucidated. We therefore investigated the effect of nutlin-3 on neointima formation.

Methods and results Nutlin-3 up-regulated p53 and its downstream target p21 in vascular smooth muscle cells (VSMCs). DNA synthesis assay and flow cytometric analysis revealed that nutlin-3 inhibited platelet-derived growth factor (PDGF)-induced VSMC proliferation by cell cycle arrest. This inhibitory effect was abrogated in p53-siRNA-transfected VSMCs. Furthermore, nutlin-3 inhibited PDGF-stimulated VSMC migration. Treatment with nutlin-3 attenuated neointimal hyperplasia at 28 days after vascular injury in mice, associated with up-regulation of p53 and p21. BrdU incorporation was decreased at 14 days after injury in nutlin-3-treated mice. TUNEL assay showed that nutlin-3 did not exaggerate apoptosis of the injured vessels. Infiltration of macrophages and T-lymphocytes and mRNA expression of chemokine (C-C motif) ligand-5, interleukin-6, and intercellular adhesion molecule-1 were decreased in the injured vessels of nutlin-3-treated mice. Nutlin-3 suppressed NF-κB activation in VSMCs, but not in p53-siRNA-transfected VSMCs.

Conclusions The MDM2 antagonist nutlin-3 inhibits VSMC proliferation, migration, and NF-κB activation, and also attenuates neointimal hyperplasia after vascular injury in mice, which is associated with suppression of vascular cell proliferation and an inflammatory response. Targeting MDM2 might be a potential therapeutic strategy for the treatment of vascular proliferative diseases.

Keywords MDM2 • p53 • Proliferation • Inflammation • Neointima

1. Introduction

Vascular proliferation and inflammation, in which vascular smooth muscle cells (VSMCs) are involved profoundly, contribute to the pathophysiology of cardiovascular diseases including atherosclerosis, post-intervention restenosis, vein bypass graft failure, and transplant vasculpoathy. Although the drug-eluting stent technology has reduced restenosis after coronary intervention, further elucidation of molecular mechanisms of vascular inflammation and proliferation is required for the retainment of vascular patency and reduction of cardiovascular events.[1–3]

The tumour protein p53 (Tp53) governs fundamental cellular processes such as apoptosis, cell cycle arrest, senescence, DNA repair, and cellular metabolism by regulating the transcription of many genes in response to stress signals.[4] p53 is believed to be involved in cardiovascular pathogenesis, however, the role of p53 in atherosclerotic diseases is Janus-faced. p53 deficiency exacerbates atherosclerosis in genetic dyslipidemic mice models,[5–8] while p53 overexpression enhances atherosclerotic plaque rupture.[9]

p53 expression is regulated by numerous proteins; more than 160 studies have been reported to date. Among them, murine double

* Corresponding author: Department of Cardiovascular Medicine, Kyushu University Graduate School of Medical Sciences, 3-1-1 Maidashi, Higashi-ku, 812-8582 Fukuoka, Japan. Tel: +81 92 642 5358; fax: +81 92 642 5374, Email: ichiki@cardiol.med.kyushu-u.ac.jp

minute 2 (MDM2) is regarded outstanding because it functions as a specific and indispensable inhibitor of p53 during embryonic development and its expression level is frequently affected in cancers.[10] MDM2 inhibits p53 transcriptional activity by occluding the transactivation domain to interrupt a recruitment of co-activators, and ubiquitinates the C-terminal domain of p53 to promote degradation by proteasome.[11]

MDM2 is overexpressed in human atherosclerotic tissues,[12] and in VSMCs of patients with primary aldosteronism,[13] indicating that MDM2 participates in pathological vascular remodelling. These studies also suggest that p53 might be suppressed by MDM2 in vascular proliferating process; therefore reactivation of the p53 pathway may be a novel therapeutic strategy for the treatment of vascular remodelling.

Disruption of the MDM2-p53 interaction has attracted an interest as a novel therapeutic strategy for cancers. Recently, a small-molecule inhibitor of MDM2-p53 binding, nutlin-3, was developed.[14] Nutlin-3 has antitumour effects by p53 activation in various cancer cells,[15] and *in vivo* administration induces tumour regression in mice.[14,16–19]

These studies prompted us to investigate the effects of nutlin-3 on vascular remodelling process, including VSMC proliferation and gene expression. In the present study, we showed that nutlin-3 inhibited platelet-derived growth factor (PDGF)-induced VSMC proliferation and NF-κB activation, and also attenuated neointimal hyperplasia after arterial injury in mice.

2. Methods

2.1 Materials

Dulbecco's modified Eagle's medium (DMEM) was purchased from Invitrogen (Carlsbad, CA, USA). Fetal bovine serum (FBS) was purchased from Nichirei Biosciences (Tokyo, Japan). Recombinant rat PDGF-BB was purchased from R&D Systems (Minneapolis, MN, USA). Bovine serum albumin (BSA), bromodeoxyuridine (BrdU), propidium iodide (PI), anti-α-tubulin antibody, and FITC-conjugated anti-α-smooth muscle actin antibody were from Sigma-Aldrich (St. Louis, MO, USA). Nutlin-3 was purchased from Cayman Chemical (Ann Arbor, MI, USA). Antibodies against p38MAPK, phospho-p38MAPK, ERK1/2, phospho-ERK1/2, JNK/SAPK, phospho-JNK/SAPK, p53, and histone H3 were purchased from Cell Signaling Technology (Beverly, MA, USA). Antibodies against p53, MDM2, PECAM-1, and Mac-3 were from Santa Cruz Biotechnology (Santa Cruz, CA, USA). Anti-p21 antibodies were from BD Biosciences Pharmingen (San Diego, CA, USA) and Imgenex (San Diego, CA, USA). Anti-CD3 antibody was from Abcam (Cambridge, MA, USA).

2.2 Cell cultures

VSMCs were isolated from the thoracic aorta of Sprague–Dawley rats (Kyudo Co., Saga, Japan). Cells were maintained in DMEM supplemented with 10% FBS at 37°C in a humidified atmosphere in 5% CO_2 in air. Before stimulation, cells were serum starved in DMEM with 0.1% BSA for 2 days.

2.3 Measurement of DNA synthesis

VSMCs pretreated with nutlin-3 (10 μmol/L) were stimulated with PDGF-BB (50 ng/mL) for 24 h and pulsed with [^{3}H]-thymidine (1 μCi/mL) for the last 6 h. Following washing with PBS, cells were incubated with 10% trichloroacetic acid, rinsed with a mixture of ethanol and diethylether (2:1), and dissolved in 0.5 N NaOH. The incorporation of [^{3}H]-thymidine into cells was measured by a liquid scintillation counter.

2.4 Flow cytometry

For cell cycle analysis, harvested VSMC were washed in PBS, and fixed in cold 70% ethanol. After treatment with RNase A (25 mg/mL) at 37°C for 60 min, cells were stained with PI (50 μg/mL) at 4°C for 30 min. Samples were analysed by BD FACSCalibur (Becton, Dickinson and Co., Franklin Lakes, NJ, USA). The cell cycle distribution was analysed by ModFit LT software (Verity Software House, Topsham, ME, USA). Apoptosis analysis was performed by using Annexin V-FITC Apoptosis Detection Kit I (BD Biosciences Pharmingen) and BD FACSCalibur according to the manufacturer's instructions.

2.5 Small-interfering RNA transfection

p53-targeting small-interfering RNA (siRNA) (#M-080060-00, a mixture of 4 siRNA: 5′ GAGAAUAUUUCACCCUUAA 3′; 5′ GCGACAGGGU CACCUAAUU 3′; 5′ GUACUCAAUUUCCCUCAAU 3′; 5′ CCACU AUCCACUACAAGUA 3′) and negative control non-targeting siRNA (D-001210-03) were purchased from Thermo Scientific Dharmacon (Lafayette, CO, USA). siRNA was introduced into VSMCs by a lipid transfection method. siRNA was mixed with lipofectamine RNAiMAX (Invitrogen, Carlsbad, CA, USA) in Opti-MEM I Reduced Serum Medium (Invitrogen) and incubated for 20 min at room temperature. VSMCs were transfected with the siRNA-lipofectamine complexes and incubated for 48 h at 37°C in a CO_2 incubator, and then used in the experiments.

2.6 Real-time reverse transcription polymerase chain reaction

Total RNA was extracted by the acid guanidinium thiocyanate–phenol chloroform extraction method. RNA was reverse transcribed using ReverTra Ace qPCR RT kit (TOYOBO, Osaka, Japan) according to the manufacturer's instructions. Real-time quantitative PCR (qPCR) was performed using THUNDERBIRD SYBR qPCR Mix (TOYOBO) and the Applied Biosystems 7500 real-time PCR system (Applied Biosystems, Foster City, CA, USA). Relative expression levels were determined by comparative Ct (ΔΔCt) method. *Hprt1* mRNA was used for standardization. Primer sequences used for amplification are as follows: <rat> *Tp53* (forward) 5′ GAGGTCGGCTCCGACTATACCA 3′, (reverse) 5′ AAAGCTGTCCCGTCCCAGAAG 3′; *Hprt1* (forward) 5′ TCCTCATG GACTGATTATGGACA 3′, (reverse) 5′ TAATCCAGCAGGTCAG CAAAGA 3′; <mouse> *Ccl5* (forward) 5′ ACCAGCAGCAAGTGC TCCAA 3′, (reverse) 5′ TGGCTAGGACTAGAGCAAGCAATG 3′; *Il6* (forward) 5′ CCACTTCACAAGTCGGAGGCTTA 3′, (reverse) 5′ GCAAGTGCATCATCGTTGTTCATAC 3′; *Icam1* (forward) 5′ GGCACCCAGCAGAAGTTGTT 3′, (reverse) 5′ CCTCAGTCACCTC TACCAAG 3′; *Hprt1* (forward) 5′ TTGTTGTTGGATATGCCCTT GACTA 3′, (reverse) 5′ AGGCAGATGGCCACAGGACTA 3′

2.7 Western blot analysis

Cells were harvested with lysis buffer composed of 1 × RIPA, 1% aprotinin, 10 μmol/L pepstatin A, 1 mmol/L PMSF, and 2.5 μg/mL leupepsin. Equal amounts of protein samples were subjected to SDS–PAGE and transferred to a polyvinylidene difluoride membrane (Immobilon-P, Millipore Corp., Billerica, MA, USA). After blocking with 5% skim milk, the membrane was incubated with a primary antibody, followed by a horseradish peroxidase (HRP)-conjugated secondary antibody. Blots were detected by chemiluminescence system using ECL Western Blotting Detection Reagent (GE Healthcare, Chalfont St Giles, UK). The membrane was exposed to X-ray film. The protein expression level was quantified by densitometry.

2.8 Cell migration assay (*in vitro* scratch assay)

VSMCs were plated onto the 35-mm dish coated with type I collagen and grown to be confluent. Following pretreatment with nutlin-3 (10 μmol/L) for 24 h, the VSMC monolayer was scraped with a pipet tip to create scratch wound, and then stimulated with PDGF-BB (50 ng/mL). After 24-h incubation, the number of cells which migrated into the scratch area was counted under microscopy.

2.9 DNA-binding ELISA for NF-κB

TransAM NF-κB p65 assay Kit (Active Motif, Carlsbad, CA, USA) was used. Equal amounts of nuclear extracts were added to the 96-well plate containing NF-κB consensus sequence and subjected to binding reaction for 1 h. Following incubation with anti-NF-κB p65 antibody for 1 h, samples were incubated with HRP-conjugated anti-IgG antibody for 1 h. Then samples were subjected to colorimetric reaction and absorbance at 450 nm was read by Mithras LB940 (Berthold Technologies, Bad Wildbad, Germany).

2.10 Animal experiments

All procedures were approved by the institutional animal use and care committee, and conducted in accordance with institutional guidelines and Guide for the Care and Use of Laboratory Animals (NIH Publication No. 85-23, revised 1996). C57B/6J male mice were purchased from CLEA Japan (Tokyo, Japan) and fed a normal chow. Mice (10-week-old) were anesthetized by intraperitoneal injection of 50 mg/kg pentobarbital, and then arterial wire injury was performed by insertion of a wire (0.38 mm in diameter. #C-SF-15-15, COOK, Bloomington, IN, USA) into the femoral artery as described previously.[20] Mini-osmotic pumps (Alzet, DURECT, Cupertino, CA, USA) delivering nutlin-3 (5 mg/kg/day) were placed into the intraperitonal space immediately after the vascular injury operation. BrdU (25 mg/kg) was injected at 24 and 1 h prior to tissue harvest. Mice were euthanized with injection of overdose pentobarbital. Harvested femoral arteries were fixed in 10% neutral-buffered formaldehyde solution. For RNA isolation, tissues were snap frozen in liquid nitrogen.

2.11 Morphometric analysis and immunohistochemistry

Neointimal and medial areas were quantified by NIH ImageJ software. Per cent stenosis was determined as the ratio of the intimal area and the area inside the internal elastic lamina × 100. For enzyme immunohistochemistry, paraffin-embedded tissue sections were deparaffinized and rehydrated, and then autoclaved in 10 mmol/L citrate buffer for antigen retrieval. Following quenching endogenous peroxidase and blocking with 3% skim milk, sections were incubated with primary antibodies at 4°C overnight. After incubation with biotinylated secondary antibodies and treatment with streptavidine-horseradish peroxidase conjugate, sections were incubated in 3,3′-diaminobenzidine solution and counterstained with haematoxylin. For fluorescent immunohistochemistry, sections were incubated with FITC-conjugated primary antibodies for 2 h at room temperature and then observed by fluorescent microscopy. Apoptotic cells were detected by the terminal deoxynucleotidyl transferase dUTP nick-end labelling (TUNEL) method with Apoptosis *in situ* Detection Kit (Wako Pure Chemical Industries, Osaka, Japan). Incorporated BrdU was detected using Cell Proliferation Kit (GE Healthcare UK).

2.12 Statistical analysis

Experimental data were analysed by one-way ANOVA and Fisher's *post hoc* test. Results are expressed as mean ± SEM. Values of $P < 0.05$ were considered statistically significant.

3. Results

3.1 Nutlin-3 activates p53 pathway and inhibits cellular proliferation and migration in VSMCs

At first, the effect of nutlin-3 on rat VSMC proliferation was examined. DNA synthesis assay showed that enhanced [^{3}H]-thymidine uptake induced by PDGF was dose dependently suppressed by nutlin-3 treatment in VSMCs (*Figure 1A*). We further assessed the effects of nutlin-3 on VSMC migration by *in vitro* scratch assay. Treatment with nutlin-3 attenuated VSMC migration induced by PDGF (*Figure 1B*).

We next verified whether nutlin-3 induces p53 in VSMCs. p53 protein expression was up-regulated by treatment with nutlin-3 (*Figure 1C*). p21 and MDM2, p53 downstream target molecules, were also up-regulated by nutlin-3 (*Figure 1C*), indicating functional activation of the p53 pathway in VSMCs. MAP kinases are known to be important mediators of PDGF signaling pathway.[21] However, nutlin-3 had no effects on the phosphorylation of p38MAPK, ERK1/2, and JNK/SAPK stimulated by PDGF (Supplementary material online, *Figure S1*). In order to exclude the possibility that the reduction of the number of proliferating cells was caused by apoptosis, we also evaluated VSMC apoptosis by flow cytometry. Treatment with nutlin-3 did not instigate apoptosis at basal condition and did not enhance H_2O_2-induced apoptosis either (*Figure 1D*). These results imply that the inhibitory effect of nutlin-3 on VSMC proliferation may not be attributable to inhibition of MAP kinases or induction of apoptosis.

3.2 Nutlin-3 induces cell cycle arrest in a p53-dependent manner in VSMCs

The effect of nutlin-3 on the cell cycle profile in rat VSMCs was analysed by flow cytometry. To confirm whether the inhibitory effect of nutlin-3 on cell proliferation depends on p53, assays were performed with or without p53 knock down by siRNA. Transfection of p53-targeting siRNA significantly down-regulated p53 mRNA expression in VSMCs, while transfection of control siRNA did not affect p53 mRNA expression levels (*Figure 2A*). Flow cytometric analysis revealed that the increase in the proportion of S-phase and the decrease in the proportion of G1-phase induced by PDGF was attenuated by treatment with nutlin-3 in VSMCs transfected with control siRNA (*Figure 2B*), whereas nutlin-3 failed to prevent cell cycle progression stimulated by PDGF in VSMCs transfected with p53-siRNA (*Figure 2B*). The cell cycle arrest-inducing effect of nutlin-3 was also abrogated in p53-deficient mouse VSMCs (Supplementary material online, *Figure S2*). These results suggest that nutlin-3 inhibited VSMC proliferation via p53-dependent cell cycle arrest at G1 phase.

3.3 Nutlin-3 attenuates neointimal hyperplasia after vascular injury

We next explored the effects of nutlin-3 on neointimal formation in mice. Administration of nutlin-3 (5 mg/kg/day) had no apparent effects on body weight and hemodynamics including blood pressure and heart rate (data not shown). No sickness behaviour and mortality occurred during the experimental period. No apparent macroscopic organ damage and tissue abnormalities were observed in nutlin-3-administered mice. Neointimal hyperplasia provoked by arterial wire-injury was significantly attenuated in nutlin-3-treated mice compared with control mice at 28 days after injury (*Figure 3A and B*). In both groups, most of the neointimal tissues were composed of α-smooth muscle actin (α-SMA) positive VSMCs (*Figure 3C*). Sirius red staining revealed that the neointimal tissues in both groups were also abundant in collagen fibres (*Figure 3D*). The collagen fibre hues under observation by polarizing microscopy were yellowish similarly